Discrete-Time Simulation of Nonlinear Musical Circuits by Means of Physically-Interpretable Iterative Solvers – Part I: Kirchhoff Methods

Federico Fontana[1] & Alberto Bernardini[2]

[1]HCILab
University of Udine, Italy
federico.fontana@uniud.it
[2]Politecnico di Milano, Italy
alberto.bernardini@polimi.it

DAFx20in22 @ MDW, Austria

1. Instantaneous Nonlinear Feedback

2. Performance of FP and NR in KD networks

Instantaneous Nonlinearity and Feedback

- Musical analog circuit and instrument models often must account for instantaneous nonlinearity as well as feedback featured by the original design. Together they create a computational issue
- Instantaneous nonlinearity involves modeled maps

$$v = c(u) \neq m_0 u + v_0$$

- Instantaneous feedback involves modeled simultaneous signal paths

$$u(t) \longrightarrow v(t) \quad , \quad v(t) \longrightarrow u(t)$$

- Rarely the original design provides temporal delays as part of an analog circuit. A delay τ does help compute nonlinear feedback loops in the model. Ex.: analog delay lines, acoustic pipes

$$u(t) = v(t - \tau) = c\big(y(t - \tau)\big).$$

Instantaneous Nonlinearity and Feedback

- Musical analog circuit and instrument models often must account for instantaneous nonlinearity as well as feedback featured by the original design. Together they create a computational issue
- Instantaneous nonlinearity involves modeled maps

$$v = c(u) \neq m_0 u + v_0$$

- Instantaneous feedback involves modeled simultaneous signal paths

$$u(t) \longrightarrow v(t) \qquad , \qquad v(t) \longrightarrow u(t)$$

- Rarely the original design provides temporal delays as part of an analog circuit. A delay τ does help compute nonlinear feedback loops in the model. Ex.: analog delay lines, acoustic pipes

$$u(t) = v(t - \tau) = c\big(y(t - \tau)\big).$$

Instantaneous Nonlinearity and Feedback

- Musical analog circuit and instrument models often must account for instantaneous nonlinearity as well as feedback featured by the original design. Together they create a computational issue
- Instantaneous nonlinearity involves modeled maps

$$v = c(u) \neq m_0 u + v_0$$

- Instantaneous feedback involves modeled simultaneous signal paths

$$u(t) \longrightarrow v(t) \qquad , \qquad v(t) \longrightarrow u(t)$$

- Rarely the original design provides temporal delays as part of an analog circuit. A delay τ does help compute nonlinear feedback loops in the model. Ex.: analog delay lines, acoustic pipes

$$u(t) = v(t - \tau) = c\big(y(t - \tau)\big).$$

Instantaneous Nonlinearity and Feedback

- Musical analog circuit and instrument models often must account for instantaneous nonlinearity as well as feedback featured by the original design. Together they create a computational issue
- Instantaneous nonlinearity involves modeled maps

$$v = c(u) \neq m_0 u + v_0$$

- Instantaneous feedback involves modeled simultaneous signal paths

$$u(t) \longrightarrow v(t) \qquad , \qquad v(t) \longrightarrow u(t)$$

- Rarely the original design provides temporal delays as part of an analog circuit. A delay τ does help compute nonlinear feedback loops in the model. Ex.: analog delay lines, acoustic pipes

$$u(t) = v(t - \tau) = c\big(y(t - \tau)\big).$$

Modeling Instantaneous Nonlinear Feedback

Several methods have been developed across decades to model (musical) analog circuits and (musical) instruments.

- Some come up with a continuous-time model before discretization
- Some embed a discretization map operating in the temporal $(t \longrightarrow kT = k/F_S)$ or transformed $(s \longrightarrow z)$ domain as part of their definition, and come up with a discrete-time model.

Such approaches can be roughly classified based on their approach:

- Multimensional *shear* of a time-domain system (2000)
- Transformations of a state-space formulation of the equation system, in the temporal (2015) or transformed domain (2003)
- Wave decomposition of the original equation system, mainly Wave Digital (WD) Filters (1989) or Digital Waveguide Filters (1993)
- Energy-based (Hamiltonian)
- Approximations (linerizations, inclusion of fictitious delays. . .).

Modeling Instantaneous Nonlinear Feedback

Several methods have been developed across decades to model (musical) analog circuits and (musical) instruments.

- Some come up with a continuous-time model before discretization
- Some embed a discretization map operating in the temporal ($t \longrightarrow kT = k/F_S$) or transformed ($s \longrightarrow z$) domain as part of their definition, and come up with a discrete-time model.

Such approaches can be roughly classified based on their approach:

- Multimensional *shear* of a time-domain system (2000)
- Transformations of a state-space formulation of the equation system, in the temporal (2015) or transformed domain (2003)
- Wave decomposition of the original equation system, mainly Wave Digital (WD) Filters (1989) or Digital Waveguide Filters (1993)
- Energy-based (Hamiltonian)
- Approximations (linerizations, inclusion of fictitious delays. . .).

Modeling Instantaneous Nonlinear Feedback

Several methods have been developed across decades to model (musical) analog circuits and (musical) instruments.

- Some come up with a continuous-time model before discretization
- Some embed a discretization map operating in the temporal $(t \longrightarrow kT = k/F_S)$ or transformed $(s \longrightarrow z)$ domain as part of their definition, and come up with a discrete-time model.

Such approaches can be roughly classified based on their approach:

- Multimensional *shear* of a time-domain system (2000)
- Transformations of a state-space formulation of the equation system, in the temporal (2015) or transformed domain (2003)
- Wave decomposition of the original equation system, mainly Wave Digital (WD) Filters (1989) or Digital Waveguide Filters (1993)
- Energy-based (Hamiltonian)
- Approximations (linerizations, inclusion of fictitious delays. . .).

Modeling Instantaneous Nonlinear Feedback

Several methods have been developed across decades to model (musical) analog circuits and (musical) instruments.

- Some come up with a continuous-time model before discretization
- Some embed a discretization map operating in the temporal $(t \longrightarrow kT = k/F_S)$ or transformed $(s \longrightarrow z)$ domain as part of their definition, and come up with a discrete-time model.

Such approaches can be roughly classified based on their approach:

- Multimensional *shear* of a time-domain system (2000)
- Transformations of a state-space formulation of the equation system, in the temporal (2015) or transformed domain (2003)
- Wave decomposition of the original equation system, mainly Wave Digital (WD) Filters (1989) or Digital Waveguide Filters (1993)
- Energy-based (Hamiltonian)
- Approximations (linerizations, inclusion of fictitious delays. . .).

Modeling Instantaneous Nonlinear Feedback

Several methods have been developed across decades to model (musical) analog circuits and (musical) instruments.

- Some come up with a continuous-time model before discretization
- Some embed a discretization map operating in the temporal ($t \longrightarrow kT = k/F_S$) or transformed ($s \longrightarrow z$) domain as part of their definition, and come up with a discrete-time model.

Such approaches can be roughly classified based on their approach:

- Multimensional *shear* of a time-domain system (2000)
- Transformations of a state-space formulation of the equation system, in the temporal (2015) or transformed domain (2003)
- Wave decomposition of the original equation system, mainly Wave Digital (WD) Filters (1989) or Digital Waveguide Filters (1993)
- Energy-based (Hamiltonian)
- Approximations (linerizations, inclusion of fictitious delays. . .).

Modeling Instantaneous Nonlinear Feedback

Several methods have been developed across decades to model (musical) analog circuits and (musical) instruments.

- Some come up with a continuous-time model before discretization
- Some embed a discretization map operating in the temporal ($t \longrightarrow kT = k/F_S$) or transformed ($s \longrightarrow z$) domain as part of their definition, and come up with a discrete-time model.

Such approaches can be roughly classified based on their approach:

- Multimensional *shear* of a time-domain system (2000)
- Transformations of a state-space formulation of the equation system, in the temporal (2015) or transformed domain (2003)
- Wave decomposition of the original equation system, mainly Wave Digital (WD) Filters (1989) or Digital Waveguide Filters (1993)
- Energy-based (Hamiltonian)
- Approximations (linerizations, inclusion of fictitious delays. . .).

Modeling Instantaneous Nonlinear Feedback

Several methods have been developed across decades to model (musical) analog circuits and (musical) instruments.

- Some come up with a continuous-time model before discretization
- Some embed a discretization map operating in the temporal $(t \longrightarrow kT = k/F_S)$ or transformed $(s \longrightarrow z)$ domain as part of their definition, and come up with a discrete-time model.

Such approaches can be roughly classified based on their approach:

- Multimensional *shear* of a time-domain system (2000)
- Transformations of a state-space formulation of the equation system, in the temporal (2015) or transformed domain (2003)
- Wave decomposition of the original equation system, mainly Wave Digital (WD) Filters (1989) or Digital Waveguide Filters (1993)
- Energy-based (Hamiltonian)
- Approximations (linerizations, inclusion of fictitious delays. . .).

Computing Instantaneous Nonlinear Feedback

Here we are not surveying existing modeling methods! We will be instead surveying our recent research results on how numerical solvers perform on a circuit/instrument model, and how they possibly back-propagate to the modeling of a digital structure. Why?

- Numerical solvers are often chosen by experts' intuition or after brute force simulations
- They undergo some informal confabulation ("Newton-Raphson wins over Fixed-Point")
- Rarely a performance analysis is made before simulations.

Specifically, we will investigate established solvers such as Fixed-Point (FP) and Newton-Raphson (NR) in both Kirchhoff (digital, KD) and WD filter networks (later on this screen by Alberto B.): the latter can be linked to a physical interpretation.

Computing Instantaneous Nonlinear Feedback

Here we are not surveying existing modeling methods! We will be instead surveying our recent research results on how numerical solvers perform on a circuit/instrument model, and how they possibly back-propagate to the modeling of a digital structure. Why?

- Numerical solvers are often chosen by experts' intuition or after brute force simulations
- They undergo some informal confabulation ("Newton-Raphson wins over Fixed-Point")
- Rarely a performance analysis is made before simulations.

Specifically, we will investigate established solvers such as Fixed-Point (FP) and Newton-Raphson (NR) in both Kirchhoff (digital, KD) and WD filter networks (later on this screen by Alberto B.): the latter can be linked to a physical interpretation.

Computing Instantaneous Nonlinear Feedback

Here we are not surveying existing modeling methods! We will be instead surveying our recent research results on how numerical solvers perform on a circuit/instrument model, and how they possibly back-propagate to the modeling of a digital structure. Why?

- Numerical solvers are often chosen by experts' intuition or after brute force simulations
- They undergo some informal confabulation ("Newton-Raphson wins over Fixed-Point")
- Rarely a performance analysis is made before simulations.

Specifically, we will investigate established solvers such as Fixed-Point (FP) and Newton-Raphson (NR) in both Kirchhoff (digital, KD) and WD filter networks (later on this screen by Alberto B.): the latter can be linked to a physical interpretation.

Focus of this tutorial

Computation of KD and WD filter networks using FP and NR solvers.

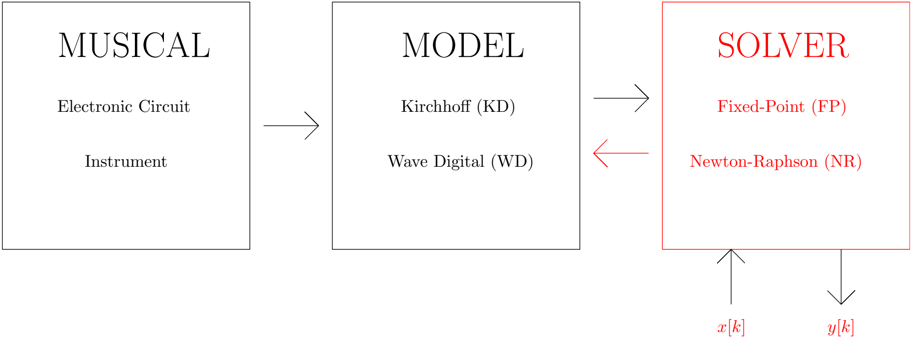

We will show that

- some quantitative preliminary analyses can be performed
- they lead to results having general validity.

Focus of this tutorial

Computation of KD and WD filter networks using FP and NR solvers.

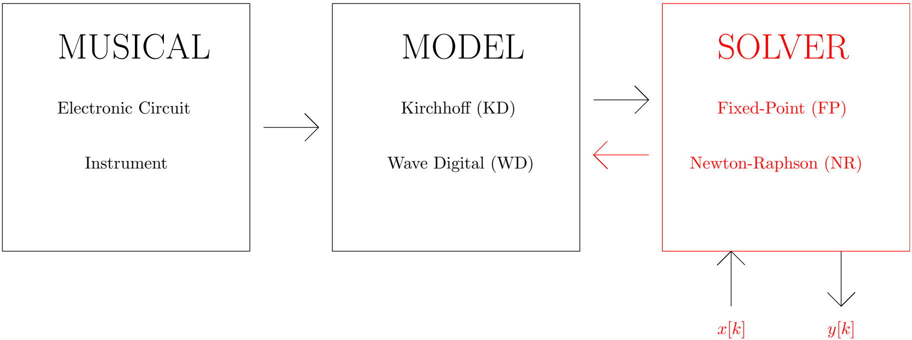

We will show that

- some quantitative preliminary analyses can be performed
- they lead to results having general validity.

Current scope and limitations

Linear blocks (i.e., digital filters) can be seen as a particular case.

$\boldsymbol{u} = [u_1 \ \ldots \ u_N]^T$ external (also null) inputs to a network, including contributions from linear blocks with memory
$\boldsymbol{v} = [v_1 \ \ldots \ v_N]^T$ outputs from the same network.

N nonlinear scalar maps $\boldsymbol{c} = [c_1, \ldots, c_N]^T$: $c_i(\boldsymbol{v}) = \sum_{j=1}^{N} c_{i,j}(v_j)$.

$\boldsymbol{F_u}$ topological description from inputs to nonlinear maps
$\boldsymbol{F_v}$ topological description of the network (map-to-map connections).

Hence, a network containing instantaneous nonlinear feedback is described by this general equation:

$$\boldsymbol{v} = \boldsymbol{F_v}\boldsymbol{c}(\boldsymbol{v}) + \boldsymbol{F_u}\boldsymbol{u}.$$

Note: Local vector nonlinear maps — e.g. signal product, transistors: $c_i(\boldsymbol{v}) = v_h \cdot v_k$ — can still be managed. (Ongoing research.)

FP $\longleftrightarrow$ KD: FP solution of a KD network

- At every time step kT, system $\boldsymbol{v}[k] = \boldsymbol{F_v c}(\boldsymbol{v}[k]) + \boldsymbol{F_u u}[k]$ must be satisfied—provided it can be (a modeling issue).
- FP simply asks to iterate at every time step along index γ:

$$\boldsymbol{v}^{(\gamma+1)}[k] = \boldsymbol{F_v c}(\boldsymbol{v}^{(\gamma)}[k]) + \boldsymbol{F_u u}[k]$$

until $\boldsymbol{v}^{(\gamma+1)}[k] \approx \boldsymbol{v}^{(\gamma)}[k]$ (the stop condition).

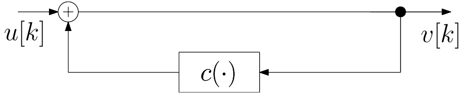

FP just asks to *follow* the signal flow

- Valuable at design stage
- Efficient implementation on cheap DSP (IoT, local memory)
- Easy to program: apply nonlinear map to $\boldsymbol{v}$ and sum $\boldsymbol{u}$; if stop condition is not met then repeat.

FP $\longleftrightarrow$ KD: FP solution of a KD network

- At every time step kT, system $\boldsymbol{v}[k] = \boldsymbol{F_v c}(\boldsymbol{v}[k]) + \boldsymbol{F_u u}[k]$ must be satisfied—provided it can be (a modeling issue).
- FP simply asks to iterate at every time step along index γ:

$$\boldsymbol{v}^{(\gamma+1)}[k] = \boldsymbol{F_v c}(\boldsymbol{v}^{(\gamma)}[k]) + \boldsymbol{F_u u}[k]$$

until $\boldsymbol{v}^{(\gamma+1)}[k] \approx \boldsymbol{v}^{(\gamma)}[k]$ (the stop condition).

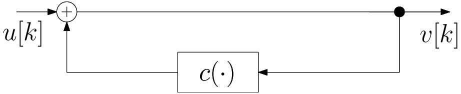

FP just asks to *follow* the signal flow

- Valuable at design stage
- Efficient implementation on cheap DSP (IoT, local memory)
- Easy to program: apply nonlinear map to $\boldsymbol{v}$ and sum $\boldsymbol{u}$; if stop condition is not met then repeat.

FP $\longleftrightarrow$ KD: FP solution of a KD network

- At every time step kT, system $\boldsymbol{v}[k] = \boldsymbol{F_v c}(\boldsymbol{v}[k]) + \boldsymbol{F_u u}[k]$ must be satisfied—provided it can be (a modeling issue).
- FP simply asks to iterate at every time step along index γ:

$$\boldsymbol{v}^{(\gamma+1)}[k] = \boldsymbol{F_v c}(\boldsymbol{v}^{(\gamma)}[k]) + \boldsymbol{F_u u}[k]$$

until $\boldsymbol{v}^{(\gamma+1)}[k] \approx \boldsymbol{v}^{(\gamma)}[k]$ (the stop condition).

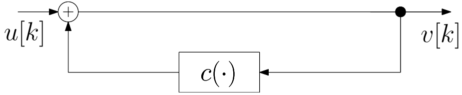

FP just asks to *follow* the signal flow

- Valuable at design stage
- Efficient implementation on cheap DSP (IoT, local memory)
- Easy to program: apply nonlinear map to $\boldsymbol{v}$ and sum $\boldsymbol{u}$; if stop condition is not met then repeat.

FP $\longleftrightarrow$ KD: FP solution of a KD network

- At every time step kT, system $\boldsymbol{v}[k] = \boldsymbol{F_v c}(\boldsymbol{v}[k]) + \boldsymbol{F_u u}[k]$ must be satisfied—provided it can be (a modeling issue).
- FP simply asks to iterate at every time step along index γ:

$$\boldsymbol{v}^{(\gamma+1)}[k] = \boldsymbol{F_v c}(\boldsymbol{v}^{(\gamma)}[k]) + \boldsymbol{F_u u}[k]$$

until $\boldsymbol{v}^{(\gamma+1)}[k] \approx \boldsymbol{v}^{(\gamma)}[k]$ (the stop condition).

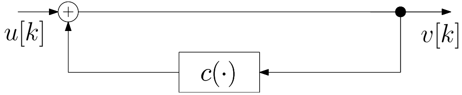

FP just asks to *follow* the signal flow

- Valuable at design stage
- Efficient implementation on cheap DSP (IoT, local memory)
- Easy to program: apply nonlinear map to $\boldsymbol{v}$ and sum $\boldsymbol{u}$; if stop condition is not met then repeat.

FP $\longleftrightarrow$ KD: FP solution of a KD network

- At every time step kT, system $\boldsymbol{v}[k] = \boldsymbol{F_v c}(\boldsymbol{v}[k]) + \boldsymbol{F_u u}[k]$ must be satisfied—provided it can be (a modeling issue).
- FP simply asks to iterate at every time step along index γ:

$$\boldsymbol{v}^{(\gamma+1)}[k] = \boldsymbol{F_v c}(\boldsymbol{v}^{(\gamma)}[k]) + \boldsymbol{F_u u}[k]$$

until $\boldsymbol{v}^{(\gamma+1)}[k] \approx \boldsymbol{v}^{(\gamma)}[k]$ (the stop condition).

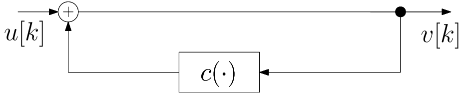

FP just asks to *follow* the signal flow

- Valuable at design stage
- Efficient implementation on cheap DSP (IoT, local memory)
- Easy to program: apply nonlinear map to $\boldsymbol{v}$ and sum $\boldsymbol{u}$; if stop condition is not met then repeat.

Condition for FP solution

- Linear case (e.g. linear filters): iteration $\boldsymbol{v}^{(\gamma+1)} = \boldsymbol{A}\boldsymbol{v}^{(\gamma)} + \boldsymbol{x}$ converges if and only if the spectral radius $\rho(\boldsymbol{A})$ is such that $\rho(\boldsymbol{A}) < 1$.
- For every k, γ we define a vector function $\boldsymbol{h}(\boldsymbol{v}) = \boldsymbol{F_v}\boldsymbol{c}(\boldsymbol{v}) + \boldsymbol{F_u}\boldsymbol{u}$ such that the spectral radius of the Jacobian matrix $\boldsymbol{J_h}(\boldsymbol{v}) = [h'_{i,j}(v_j)]$ of $\boldsymbol{h}(\boldsymbol{v})$ is less than one:

$$\rho(\boldsymbol{J_h}(\boldsymbol{v})) < 1$$

- Common practice: find $\boldsymbol{A}$ such that $\rho(\boldsymbol{J_h}(\boldsymbol{v})) \leq \rho(\boldsymbol{A}) < 1$
- Note: upper bounds provide sufficient conditions (sometimes too strong!).

Condition for FP solution

- Linear case (e.g. linear filters): iteration $\boldsymbol{v}^{(\gamma+1)} = \boldsymbol{A}\boldsymbol{v}^{(\gamma)} + \boldsymbol{x}$ converges if and only if the spectral radius $\rho(\boldsymbol{A})$ is such that $\rho(\boldsymbol{A}) < 1$.
- For every k, γ we define a vector function $\boldsymbol{h}(\boldsymbol{v}) = \boldsymbol{F_v}\boldsymbol{c}(\boldsymbol{v}) + \boldsymbol{F_u}\boldsymbol{u}$ such that the spectral radius of the Jacobian matrix $\boldsymbol{J_h}(\boldsymbol{v}) = [h'_{i,j}(v_j)]$ of $\boldsymbol{h}(\boldsymbol{v})$ is less than one:

$$\rho\big(\boldsymbol{J_h}(\boldsymbol{v})\big) < 1$$

- Common practice: find $\boldsymbol{A}$ such that $\rho\big(\boldsymbol{J_h}(\boldsymbol{v})\big) \leq \rho(\boldsymbol{A}) < 1$
- Note: upper bounds provide sufficient conditions (sometimes too strong!).

Condition for FP solution

- Linear case (e.g. linear filters): iteration $\boldsymbol{v}^{(\gamma+1)} = \boldsymbol{A}\boldsymbol{v}^{(\gamma)} + \boldsymbol{x}$ converges if and only if the spectral radius $\rho(\boldsymbol{A})$ is such that $\rho(\boldsymbol{A}) < 1$.
- For every k, γ we define a vector function $\boldsymbol{h}(\boldsymbol{v}) = \boldsymbol{F_v}\boldsymbol{c}(\boldsymbol{v}) + \boldsymbol{F_u}\boldsymbol{u}$ such that the spectral radius of the Jacobian matrix $\boldsymbol{J_h}(\boldsymbol{v}) = [h'_{i,j}(v_j)]$ of $\boldsymbol{h}(\boldsymbol{v})$ is less than one:

$$\rho\big(\boldsymbol{J_h}(\boldsymbol{v})\big) < 1$$

- Common practice: find $\boldsymbol{A}$ such that $\rho\big(\boldsymbol{J_h}(\boldsymbol{v})\big) \leq \rho(\boldsymbol{A}) < 1$
- Note: upper bounds provide sufficient conditions (sometimes too strong!).

Condition for FP solution

- Linear case (e.g. linear filters): iteration $\boldsymbol{v}^{(\gamma+1)} = \boldsymbol{A}\boldsymbol{v}^{(\gamma)} + \boldsymbol{x}$ converges if and only if the spectral radius $\rho(\boldsymbol{A})$ is such that $\rho(\boldsymbol{A}) < 1$.
- For every k, γ we define a vector function $\boldsymbol{h}(\boldsymbol{v}) = \boldsymbol{F}_{\boldsymbol{v}}\boldsymbol{c}(\boldsymbol{v}) + \boldsymbol{F}_{\boldsymbol{u}}\boldsymbol{u}$ such that the spectral radius of the Jacobian matrix $\boldsymbol{J}_{\boldsymbol{h}}(\boldsymbol{v}) = [h'_{i,j}(v_j)]$ of $\boldsymbol{h}(\boldsymbol{v})$ is less than one:

$$\rho\big(\boldsymbol{J}_{\boldsymbol{h}}(\boldsymbol{v})\big) < 1$$

- Common practice: find $\boldsymbol{A}$ such that $\rho\big(\boldsymbol{J}_{\boldsymbol{h}}(\boldsymbol{v})\big) \leq \rho(\boldsymbol{A}) < 1$
- Note: upper bounds provide sufficient conditions (sometimes too strong!).

Example: EMS VCS3 VCF model (2008)

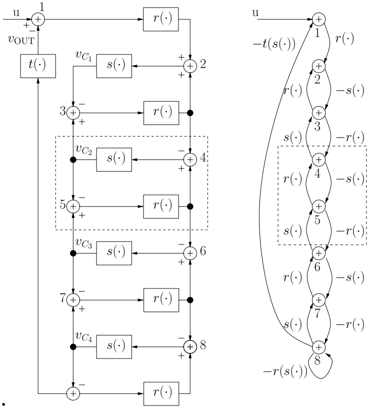

$$
\begin{cases}
\dot{v}_{C_1} = \frac{I_0}{2C}\left(\tanh\frac{u-v_{\mathrm{OUT}}}{2V_T} + \tanh\frac{v_{C_2}-v_{C_1}}{2\sigma}\right)\\
\dot{v}_{C_2} = \frac{I_0}{2C}\left(\tanh\frac{v_{C_3}-v_{C_2}}{2\sigma} - \tanh\frac{v_{C_2}-v_{C_1}}{2\sigma}\right)\\
\dot{v}_{C_3} = \frac{I_0}{2C}\left(\tanh\frac{v_{C_4}-v_{C_3}}{2\sigma} - \tanh\frac{v_{C_3}-v_{C_2}}{2\sigma}\right)\\
\dot{v}_{C_4} = \frac{I_0}{2C}\left(-\tanh\frac{v_{C_4}}{6\sigma} - \tanh\frac{v_{C_4}-v_{C_3}}{2\sigma}\right)\\
v_{OUT} = \frac{2R_2+R_1}{2R_1}\, v_{C_4} = (K+1/2)\, v_{C_4}
\end{cases}
.
$$

EMS VCF - An upper bounding matrix

Bounding hyperbolic tangents (nonlinear filter blocks $r(\cdot), s(\cdot), t(\cdot)$) with straight lines:

$$|r(u)| \le r|u| \quad , \quad |s(u)| \le s|u| \quad , \quad |t(u)| \le t|u|$$

$$\boldsymbol{A}_{\mathrm{VCF}} = \begin{bmatrix} 0 & 0 & 0 & 0 & 0 & 0 & 0 & -ts \\ r & 0 & r & 0 & 0 & 0 & 0 & 0 \\ 0 & -s & 0 & s & 0 & 0 & 0 & 0 \\ 0 & 0 & -r & 0 & r & 0 & 0 & 0 \\ 0 & 0 & 0 & -s & 0 & s & 0 & 0 \\ 0 & 0 & 0 & 0 & -r & 0 & r & 0 \\ 0 & 0 & 0 & 0 & 0 & -s & 0 & s \\ 0 & 0 & 0 & 0 & 0 & 0 & -r & -rs \end{bmatrix} .$$

$$\det(\boldsymbol{A}_{\mathrm{VCF}}) = (ts)r(rs)^{N/2-1} = (rs)^{N/2}t$$

Check whether its roots are such that $|rs|^{N/2}|t| < 1$, or $|rs| < |t|^{-N/2}$.

FP convergence speed in the EMS VCF

Critical VCS3 VCF resonance frequency and feedback gain parameters $r = 1$, $s = 1500/F_S$, and $t = 10$ for FP convergence speed correspond to ($N = 8$)

$$|rs|^{N/2}|t| \approx 10^{-5}$$

when the model runs at $F_S = 44.1$ kHz.

A more elaborate upper bound condition which applies the Gershgorin theorem to $\boldsymbol{A}_{\mathrm{VCF}}$ shows that

- FP is highly sensitive to changes in the resonance parameter
- FP convergence is guaranteed for *every* choice of the EMS VCS3 control parameters if $\phi \lessapprox \sqrt{\frac{577 \cdot 10^3}{F_S}}$, with ϕ the radius of the largest Gershgorin disk (FP convergence if $0 \leq \phi < 1$).

FP convergence speed in the EMS VCF

Critical VCS3 VCF resonance frequency and feedback gain parameters $r = 1$, $s = 1500/F_S$, and $t = 10$ for FP convergence speed correspond to ($N = 8$)

$$|rs|^{N/2}|t| \approx 10^{-5}$$

when the model runs at $F_S = 44.1$ kHz.

A more elaborate upper bound condition which applies the Gershgorin theorem to $\boldsymbol{A}_{\mathrm{VCF}}$ shows that

- FP is highly sensitive to changes in the resonance parameter
- FP convergence is guaranteed for *every* choice of the EMS VCS3 control parameters if $\phi \lessapprox \sqrt{\frac{577\cdot 10^3}{F_S}}$, with ϕ the radius of the largest Gershgorin disk (FP convergence if $0 \leq \phi < 1$).

Example: Ring Modulator (RM) model

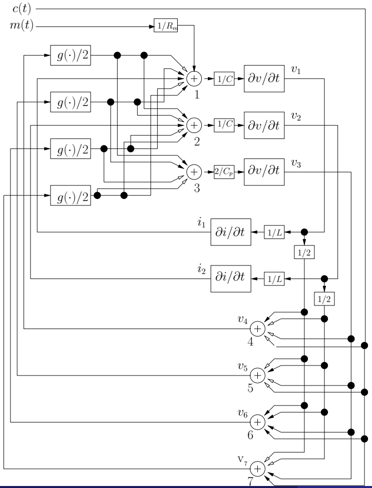

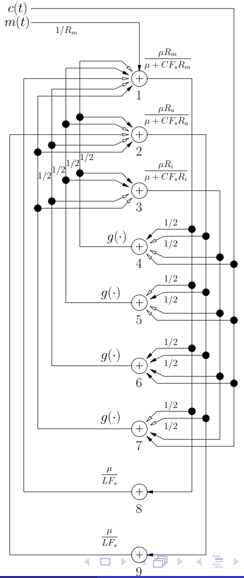

RM - An upper bounding matrix

This time the Jacobian matrix depends on the signal differences!

$$
\boldsymbol{J}_{\mathrm{RM}}(\Xi) = \begin{bmatrix}
0 & 0 & 0 & -\frac{\rho_m g'(\xi_{1,4})}{2} & \frac{\rho_m g'(\xi_{1,5})}{2} & -\frac{\rho_m g'(\xi_{1,6})}{2} & \frac{\rho_m g'(\xi_{1,7})}{2} & \rho_m & 0 \\
0 & 0 & 0 & \frac{\rho_a g'(\xi_{2,4})}{2} & -\frac{\rho_a g'(\xi_{2,5})}{2} & -\frac{\rho_a g'(\xi_{2,6})}{2} & \frac{\rho_a g'(\xi_{2,7})}{2} & 0 & \rho_a \\
0 & 0 & 0 & \rho_i g'(\xi_{3,4}) & \rho_i g'(\xi_{3,5}) & -\rho_i g'(\xi_{3,6}) & -\rho_i g'(\xi_{3,7}) & 0 & 0 \\
1/2 & -1/2 & -1 & 0 & 0 & 0 & 0 & 0 & 0 \\
-1/2 & 1/2 & -1 & 0 & 0 & 0 & 0 & 0 & 0 \\
1/2 & 1/2 & 1 & 0 & 0 & 0 & 0 & 0 & 0 \\
-1/2 & -1/2 & 1 & 0 & 0 & 0 & 0 & 0 & 0 \\
-\frac{\mu}{LF_S} & 0 & 0 & 0 & 0 & 0 & 0 & 0 & 0 \\
0 & -\frac{\mu}{LF_S} & 0 & 0 & 0 & 0 & 0 & 0 & 0
\end{bmatrix}
$$

with

- $g(\cdot)$ diode conductance,
- $u_j \leq \xi_{i,j} \leq v_j$ such that $g_i(\boldsymbol{u}) - g_i(\boldsymbol{v}) = \sum_{j=1}^{N} g'_{i,j}(\xi_{i,j})(u_j - v_j)$,
- $\mu = 1$ for backward Euler, $\mu = 1/2$ for trapezoidal rule during finite differentiation.

FP convergence speed in the RM

After some algebra around the Gershgorin disks:

$$\|g'\|_\infty \leq \frac{\phi^2}{8}\left(\frac{1}{R_i} + \frac{C_p F_S}{\mu}\right).$$

Observations:

- larger voltage amplitudes rapidly increase g', pushing FP toward divergence unless F_S is further increased
- at high F_S the above bound depends on the product $\phi^2 C_p F_S/\mu$. This means that faster convergence afforded by smaller ϕ values results in smaller ranges of convergence as a side effect. In practice we expect that higher rates may accelerate speed, however with no benefit for FP stability
- almost no effect of the finite difference scheme choice.

FP convergence speed in the RM

After some algebra around the Gershgorin disks:

$$\|g'\|_\infty \leq \frac{\phi^2}{8}\left(\frac{1}{R_i} + \frac{C_p F_S}{\mu}\right).$$

Observations:

- larger voltage amplitudes rapidly increase g', pushing FP toward divergence unless F_S is further increased
- at high F_S the above bound depends on the product $\phi^2 C_p F_S/\mu$. This means that faster convergence afforded by smaller ϕ values results in smaller ranges of convergence as a side effect. In practice we expect that higher rates may accelerate speed, however with no benefit for FP stability
- almost no effect of the finite difference scheme choice.

FP convergence speed in the RM

After some algebra around the Gershgorin disks:

$$\|g'\|_\infty \leq \frac{\phi^2}{8}\left(\frac{1}{R_i} + \frac{C_p F_S}{\mu}\right).$$

Observations:

- larger voltage amplitudes rapidly increase g', pushing FP toward divergence unless F_S is further increased
- at high F_S the above bound depends on the product $\phi^2 C_p F_S/\mu$. This means that faster convergence afforded by smaller ϕ values results in smaller ranges of convergence as a side effect. In practice we expect that higher rates may accelerate speed, however with no benefit for FP stability
- almost no effect of the finite difference scheme choice.

RM: simulations using FP, also with forced stop $\gamma = 0$

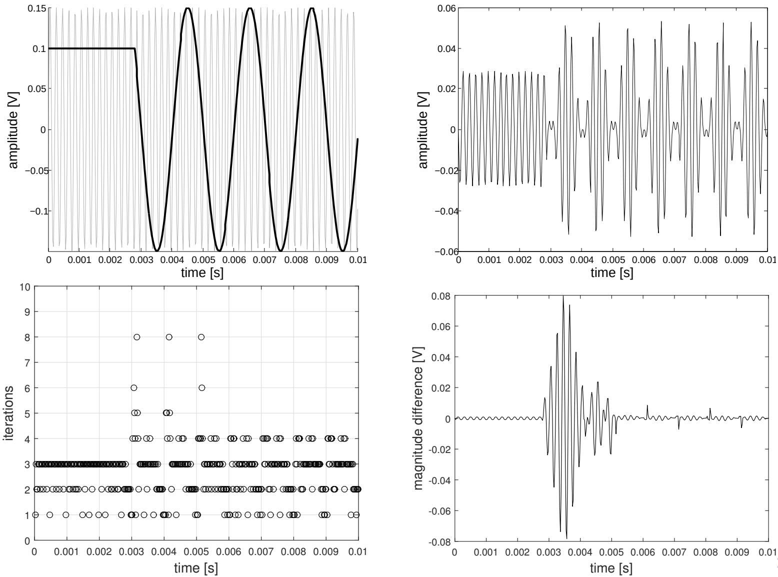

NR $\longleftrightarrow$ KD: NR solution of a KD network

- NR finds a root of $f(v)$ by iterating along γ: $v^{(\gamma+1)} = v^{(\gamma)} - \frac{f(v^{(\gamma)})}{f'(v^{(\gamma)})}$.
- Provided $\boldsymbol{v}[k] = \boldsymbol{F}_v \boldsymbol{d}(\boldsymbol{v}[k]) + \boldsymbol{F}_u \boldsymbol{u}[k] = \boldsymbol{c}(\boldsymbol{v}[k]) + \boldsymbol{x}[k]$ at every time step kT, we can look for a zero of the function $\boldsymbol{f}(\boldsymbol{v}) = \boldsymbol{v} - \boldsymbol{c}(\boldsymbol{v}) - \boldsymbol{x}$ by computing and then evaluating at every γ the inverse of $\boldsymbol{J}_f(\boldsymbol{v}^{(\gamma)}) = \boldsymbol{I} - \boldsymbol{J}_c(\boldsymbol{v}^{(\gamma)})$:

$$\boldsymbol{v}^{(\gamma+1)} = \boldsymbol{v}^{(\gamma)} - \left(\boldsymbol{I} - \boldsymbol{J}_c(\boldsymbol{v}^{(\gamma)})\right)^{-1} \left(\boldsymbol{v}^{(\gamma)} - \boldsymbol{c}(\boldsymbol{v}^{(\gamma)}) - \boldsymbol{x}\right).$$

- Note: $v^{(\gamma+1)} = v^{(\gamma)} - \frac{v^{(\gamma)} - c(v^{(\gamma)}) - x}{1 - c'(v^{(\gamma+1)})} = \frac{c(v^{(\gamma)}) - c'(v^{(\gamma)})v^{(\gamma)} + x}{1 - c'(v^{(\gamma)})}$, i.e.,

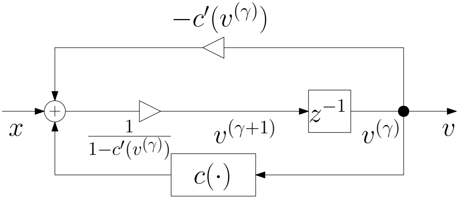

NR belongs to the fixed-point scheme family

NR $\longleftrightarrow$ KD: NR solution of a KD network

- NR finds a root of $f(v)$ by iterating along γ: $v^{(\gamma+1)} = v^{(\gamma)} - \frac{f(v^{(\gamma)})}{f'(v^{(\gamma)})}$.
- Provided $\boldsymbol{v}[k] = \boldsymbol{F_v}\boldsymbol{d}(\boldsymbol{v}[k]) + \boldsymbol{F_u}\boldsymbol{u}[k] = \boldsymbol{c}(\boldsymbol{v}[k]) + \boldsymbol{x}[k]$ at every time step kT, we can look for a zero of the function $\boldsymbol{f}(\boldsymbol{v}) = \boldsymbol{v} - \boldsymbol{c}(\boldsymbol{v}) - \boldsymbol{x}$ by computing and then evaluating at every γ the inverse of $\boldsymbol{J}_f(\boldsymbol{v}^{(\gamma)}) = \boldsymbol{I} - \boldsymbol{J}_c(\boldsymbol{v}^{(\gamma)})$:

$$\boldsymbol{v}^{(\gamma+1)} = \boldsymbol{v}^{(\gamma)} - \left(\boldsymbol{I} - \boldsymbol{J}_c(\boldsymbol{v}^{(\gamma)})\right)^{-1}\left(\boldsymbol{v}^{(\gamma)} - \boldsymbol{c}(\boldsymbol{v}^{(\gamma)}) - \boldsymbol{x}\right).$$

- Note: $v^{(\gamma+1)} = v^{(\gamma)} - \frac{v^{(\gamma)} - c(v^{(\gamma)}) - x}{1 - c'(v^{(\gamma+1)})} = \frac{c(v^{(\gamma)}) - c'(v^{(\gamma)})v^{(\gamma)} + x}{1 - c'(v^{(\gamma)})}$, i.e.,

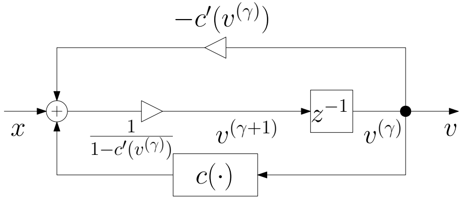

NR belongs to the fixed-point scheme family

NR ⟷ KD: NR solution of a KD network

- NR finds a root of $f(v)$ by iterating along γ: $v^{(\gamma+1)} = v^{(\gamma)} - \frac{f(v^{(\gamma)})}{f'(v^{(\gamma)})}$.
- Provided $\boldsymbol{v}[k] = \boldsymbol{F_v}\boldsymbol{d}(\boldsymbol{v}[k]) + \boldsymbol{F_u}\boldsymbol{u}[k] = \boldsymbol{c}(\boldsymbol{v}[k]) + \boldsymbol{x}[k]$ at every time step kT, we can look for a zero of the function $\boldsymbol{f}(\boldsymbol{v}) = \boldsymbol{v} - \boldsymbol{c}(\boldsymbol{v}) - \boldsymbol{x}$ by computing and then evaluating at every γ the inverse of $\boldsymbol{J}_f(\boldsymbol{v}^{(\gamma)}) = \boldsymbol{I} - \boldsymbol{J}_c(\boldsymbol{v}^{(\gamma)})$:

$$\boldsymbol{v}^{(\gamma+1)} = \boldsymbol{v}^{(\gamma)} - \left(\boldsymbol{I} - \boldsymbol{J}_c(\boldsymbol{v}^{(\gamma)})\right)^{-1}\left(\boldsymbol{v}^{(\gamma)} - \boldsymbol{c}(\boldsymbol{v}^{(\gamma)}) - \boldsymbol{x}\right).$$

- Note: $v^{(\gamma+1)} = v^{(\gamma)} - \frac{v^{(\gamma)} - c(v^{(\gamma)}) - x}{1 - c'(v^{(\gamma+1)})} = \frac{c(v^{(\gamma)}) - c'(v^{(\gamma)})v^{(\gamma)} + x}{1 - c'(v^{(\gamma)})}$, i.e.,

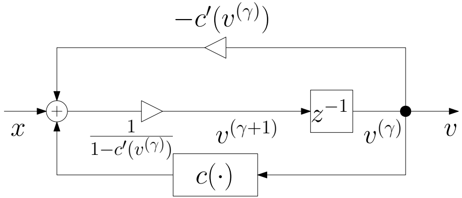

NR belongs to the fixed-point scheme family

A multidimensional basin of NR convergence

- We consider a basin such that $M\|\boldsymbol{v}-\boldsymbol{v}^{(\gamma)}\|_\infty \leq \left(M\|\boldsymbol{v}-\boldsymbol{v}^{(0)}\|_\infty\right)^{2^\gamma}$
- A solution trajectory $\boldsymbol{v}^{(\gamma)}$ falling within that basin will converge with quadratic speed to solution $\boldsymbol{v}$ — FP converges with linear speed.
- Let $\boldsymbol{H}_f(\boldsymbol{v}) = \left[f''_{i,j}(v_j)\right]$. Holding appropriate continuity, derivability, invertibility hypotheses etc. in n-D space $\mathcal{I}$ then if $\boldsymbol{v}^{(0)} \in \mathcal{I}$, $M\|\boldsymbol{v}-\boldsymbol{v}^{(0)}\|_\infty < 1$, then an NR iteration starting from $\boldsymbol{v}^{(0)}$ generates a trajectory converging to $\boldsymbol{v}$ with quadratic speed with

$$M(\boldsymbol{v}) = \frac{1}{2}\|\boldsymbol{J}_f(\boldsymbol{v})^{-1}\boldsymbol{H}_f(\boldsymbol{v})\|_\infty.$$

- A basin extension cannot be computed *before* knowing the solution $\boldsymbol{v}$. Nevertheless, $M(\boldsymbol{v})$ will be used proficiently.
- The smaller $M(\boldsymbol{v})$, the larger $\|\boldsymbol{v}-\boldsymbol{v}^{(0)}\|_\infty$ can be. The faster too??

A multidimensional basin of NR convergence

- We consider a basin such that $M\|\boldsymbol{v}-\boldsymbol{v}^{(\gamma)}\|_\infty \leq \left(M\|\boldsymbol{v}-\boldsymbol{v}^{(0)}\|_\infty\right)^{2^\gamma}$
- A solution trajectory $\boldsymbol{v}^{(\gamma)}$ falling within that basin will converge with quadratic speed to solution $\boldsymbol{v}$ — FP converges with linear speed.
- Let $\boldsymbol{H}_f(\boldsymbol{v}) = \left[f''_{i,j}(v_j)\right]$. Holding appropriate continuity, derivability, invertibility hypotheses etc. in n-D space $\mathcal{I}$ then if $\boldsymbol{v}^{(0)} \in \mathcal{I}$, $M\|\boldsymbol{v}-\boldsymbol{v}^{(0)}\|_\infty < 1$, then an NR iteration starting from $\boldsymbol{v}^{(0)}$ generates a trajectory converging to $\boldsymbol{v}$ with quadratic speed with

$$M(\boldsymbol{v}) = \frac{1}{2}\|\boldsymbol{J}_f(\boldsymbol{v})^{-1}\boldsymbol{H}_f(\boldsymbol{v})\|_\infty.$$

- A basin extension cannot be computed *before* knowing the solution $\boldsymbol{v}$. Nevertheless, $M(\boldsymbol{v})$ will be used proficiently.
- The smaller $M(\boldsymbol{v})$, the larger $\|\boldsymbol{v}-\boldsymbol{v}^{(0)}\|_\infty$ can be. The faster too??

A multidimensional basin of NR convergence

- We consider a basin such that $M\|\boldsymbol{v} - \boldsymbol{v}^{(\gamma)}\|_\infty \leq \left(M\|\boldsymbol{v} - \boldsymbol{v}^{(0)}\|_\infty\right)^{2^\gamma}$
- A solution trajectory $\boldsymbol{v}^{(\gamma)}$ falling within that basin will converge with quadratic speed to solution $\boldsymbol{v}$ — FP converges with linear speed.
- Let $\boldsymbol{H}_f(\boldsymbol{v}) = \left[f''_{i,j}(v_j)\right]$. Holding appropriate continuity, derivability, invertibility hypotheses etc. in n-D space $\mathcal{I}$ then if $\boldsymbol{v}^{(0)} \in \mathcal{I}$, $M\|\boldsymbol{v} - \boldsymbol{v}^{(0)}\|_\infty < 1$, then an NR iteration starting from $\boldsymbol{v}^{(0)}$ generates a trajectory converging to $\boldsymbol{v}$ with quadratic speed with

$$M(\boldsymbol{v}) = \frac{1}{2}\|\boldsymbol{J}_f(\boldsymbol{v})^{-1}\boldsymbol{H}_f(\boldsymbol{v})\|_\infty.$$

- A basin extension cannot be computed *before* knowing the solution $\boldsymbol{v}$. Nevertheless, $M(\boldsymbol{v})$ will be used proficiently.
- The smaller $M(\boldsymbol{v})$, the larger $\|\boldsymbol{v} - \boldsymbol{v}^{(0)}\|_\infty$ can be. The faster too??

A multidimensional basin of NR convergence

- We consider a basin such that $M\|\boldsymbol{v} - \boldsymbol{v}^{(\gamma)}\|_\infty \leq \left(M\|\boldsymbol{v} - \boldsymbol{v}^{(0)}\|_\infty\right)^{2^\gamma}$
- A solution trajectory $\boldsymbol{v}^{(\gamma)}$ falling within that basin will converge with quadratic speed to solution $\boldsymbol{v}$ — FP converges with linear speed.
- Let $\boldsymbol{H}_f(\boldsymbol{v}) = \left[f''_{i,j}(v_j)\right]$. Holding appropriate continuity, derivability, invertibility hypotheses etc. in n-D space $\mathcal{I}$ then if $\boldsymbol{v}^{(0)} \in \mathcal{I}$, $M\|\boldsymbol{v} - \boldsymbol{v}^{(0)}\|_\infty < 1$, then an NR iteration starting from $\boldsymbol{v}^{(0)}$ generates a trajectory converging to $\boldsymbol{v}$ with quadratic speed with

$$M(\boldsymbol{v}) = \frac{1}{2}\|\boldsymbol{J}_f(\boldsymbol{v})^{-1}\boldsymbol{H}_f(\boldsymbol{v})\|_\infty.$$

- A basin extension cannot be computed *before* knowing the solution $\boldsymbol{v}$. Nevertheless, $M(\boldsymbol{v})$ will be used proficiently.
- The smaller $M(\boldsymbol{v})$, the larger $\|\boldsymbol{v} - \boldsymbol{v}^{(0)}\|_\infty$ can be. The faster too??

A multidimensional basin of NR convergence

- We consider a basin such that $M\|\boldsymbol{v} - \boldsymbol{v}^{(\gamma)}\|_\infty \le \left(M\|\boldsymbol{v} - \boldsymbol{v}^{(0)}\|_\infty\right)^{2^\gamma}$
- A solution trajectory $\boldsymbol{v}^{(\gamma)}$ falling within that basin will converge with quadratic speed to solution $\boldsymbol{v}$ — FP converges with linear speed.
- Let $\boldsymbol{H}_f(\boldsymbol{v}) = \left[f''_{i,j}(v_j)\right]$. Holding appropriate continuity, derivability, invertibility hypotheses etc. in n-D space $\mathcal{I}$ then if $\boldsymbol{v}^{(0)} \in \mathcal{I}$, $M\|\boldsymbol{v} - \boldsymbol{v}^{(0)}\|_\infty < 1$, then an NR iteration starting from $\boldsymbol{v}^{(0)}$ generates a trajectory converging to $\boldsymbol{v}$ with quadratic speed with

$$M(\boldsymbol{v}) = \frac{1}{2}\|\boldsymbol{J}_f(\boldsymbol{v})^{-1}\boldsymbol{H}_f(\boldsymbol{v})\|_\infty.$$

- A basin extension cannot be computed *before* knowing the solution $\boldsymbol{v}$. Nevertheless, $M(\boldsymbol{v})$ will be used proficiently.
- The smaller $M(\boldsymbol{v})$, the larger $\|\boldsymbol{v} - \boldsymbol{v}^{(0)}\|_\infty$ can be. The faster too??

Example: Diode Clipper (DC) model

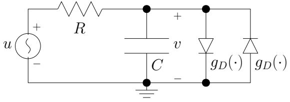

(a)

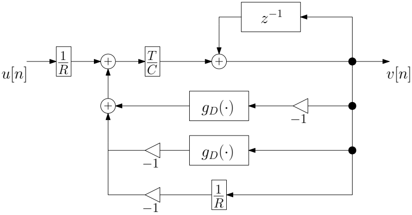

(b)

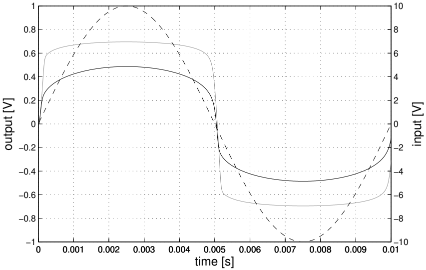

Backward Euler: $v[k] = \frac{T}{C}\left(\frac{u[k]-v[k]}{R} - g_D(v[k]) + g_D(-v[k])\right) + v[k-1]$.

Black: polynomial diode characteristic $i = g_D(v) = V_P v^4 1(v)$.

Grey: exponential diode characteristic $i = g_D(v) = I_D(e^{v/2V_E} - 1)$.

NR convergence speed in the DC

$$M(v) = \frac{1}{2}\left|\frac{f''(v)}{f'(v)}\right| = \frac{1}{2}\left|\frac{\rho\left(g_D''(v) - g_D''(-v)\right)}{1 + \rho\left(g_D'(v) + g_D'(-v)\right)}\right|$$

Strong (inverse) correlation between $M(v)$ and speed:

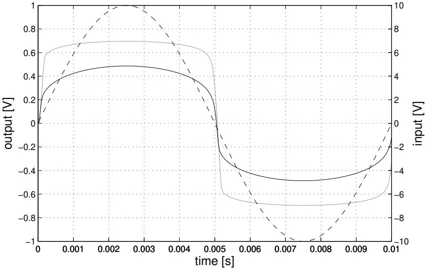

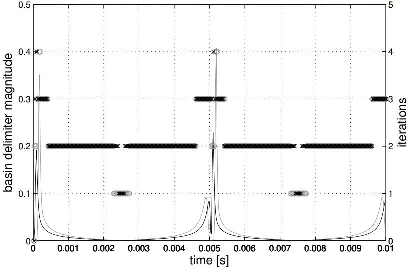

Global convergence if $M(v)$ is limited. With both diodes, two symmetric maxima equal to $M(\infty) = \frac{1}{4V_E}$ and $M\left(\sqrt[3]{\frac{1}{2\rho V_P}}\right) = \sqrt[3]{2\rho V_P}$, respectively.

Example: RM model (the same as before)

Rearranging $\boldsymbol{J}_f(\boldsymbol{v}) = \boldsymbol{I} - \boldsymbol{J}_c(\boldsymbol{v})$ — we already saw $\boldsymbol{J}_c = \boldsymbol{J}_{\mathrm{RM}}$:

$$\boldsymbol{J}_f = \begin{bmatrix} \boldsymbol{I} & \emptyset \\ -\boldsymbol{B} & \boldsymbol{I} \end{bmatrix} \begin{bmatrix} \boldsymbol{I} & \emptyset \\ \emptyset & \boldsymbol{I} - \boldsymbol{BA} \end{bmatrix} \begin{bmatrix} \boldsymbol{I} & -\boldsymbol{A} \\ \emptyset & \boldsymbol{I} \end{bmatrix},$$

with

$$\boldsymbol{A}(\boldsymbol{v}) = \begin{bmatrix} -\frac{\rho_m}{2} g_D'(v_4) & \frac{\rho_m}{2} g_D'(v_5) & -\frac{\rho_m}{2} g_D'(v_6) & \frac{\rho_m}{2} g_D'(v_7) & \rho_m & 0 \\ \frac{\rho_a}{2} g_D'(v_4) & -\frac{\rho_a}{2} g_D'(v_5) & -\frac{\rho_a}{2} g_D'(v_6) & \frac{\rho_a}{2} g_D'(v_7) & 0 & \rho_a \\ \rho_l g_D'(v_4) & \rho_l g_D'(v_5) & -\rho_l g_D'(v_6) & -\rho_l g_D'(v_7) & 0 & 0 \end{bmatrix}$$

and

$$\boldsymbol{B} = \begin{bmatrix} 1/2 & -1/2 & -1 \\ -1/2 & 1/2 & -1 \\ 1/2 & 1/2 & 1 \\ -1/2 & -1/2 & 1 \\ -\frac{1}{LF_s} & 0 & 0 \\ 0 & -\frac{1}{LF_s} & 0 \end{bmatrix}.$$

NR convergence speed in the RM: some algebra

After some algebra, here, too:

$$\boldsymbol{J}_f(\boldsymbol{v})^{-1}\boldsymbol{H}_f(\boldsymbol{v}) = \begin{bmatrix} \emptyset & (\boldsymbol{I}-\boldsymbol{AB})^{-1}\boldsymbol{C} \\ \emptyset & \boldsymbol{B}(\boldsymbol{I}-\boldsymbol{AB})^{-1}\boldsymbol{C} \end{bmatrix}$$

with

$$\boldsymbol{C}(\boldsymbol{v}) = \begin{bmatrix} -\frac{\rho_m}{2}g_D''(v_4) & \frac{\rho_m}{2}g_D''(v_5) & -\frac{\rho_m}{2}g_D''(v_6) & \frac{\rho_m}{2}g_D''(v_7) & 0 & 0 \\ \frac{\rho_a}{2}g_D''(v_4) & -\frac{\rho_a}{2}g_D''(v_5) & -\frac{\rho_a}{2}g_D''(v_6) & \frac{\rho_a}{2}g_D''(v_7) & 0 & 0 \\ \rho_l g_D''(v_4) & \rho_l g_D''(v_5) & -\rho_l g_D''(v_6) & -\rho_l g_D''(v_7) & 0 & 0 \end{bmatrix}$$

in which, using backward Euler,

$$\rho_m = \frac{R_m}{1+R_mCF_s},\ \rho_a = \frac{R_a}{1+R_aCF_s},\ \rho_l = \frac{R_l}{1+R_lC_pF_s}.$$

and, finally, $\|\boldsymbol{J}_f(\boldsymbol{v})^{-1}\boldsymbol{H}_f(\boldsymbol{v})\|_\infty = \|\boldsymbol{B}\|_\infty\|(\boldsymbol{I}-\boldsymbol{AB})^{-1}\|_\infty\|\boldsymbol{C}\|_\infty$.

NR convergence speed in the RM: results

As for FP vs. VCF, unfortunately $\|\boldsymbol{C}\|_\infty$ depends on $g_D''(v)$:

$$\|\boldsymbol{C}\|_\infty \leq 4\max\{\rho_m, \rho_a, \rho_l\}\, g_D''\Big(\max_{i=4,5,6,7}\{v_i\}\Big).$$

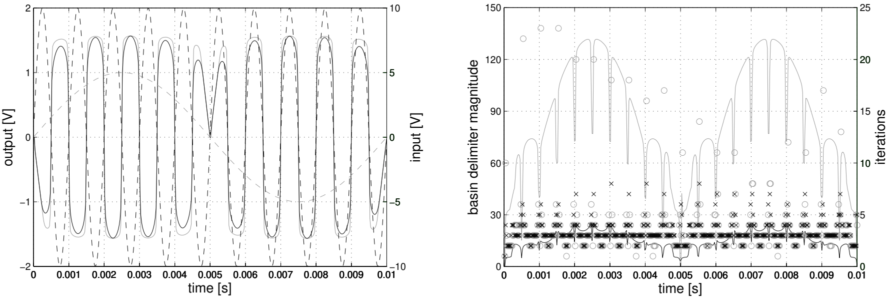

$C = C_p = 10^{-9}$ F, $L = 0.8$ H, $R_a = 600\ \Omega$, $R_i = 50\ \Omega$, $R_m = 80\ \Omega$, $F_S = 44.1$ kHz.

Intermediate conclusions (before WD)

Alberto B. will make better use of $M(\boldsymbol{v})$ shortly!

References:

- Fontana, Federico, and Enrico Bozzo. "Explicit fixed-point computation of nonlinear delay-free loop filter networks." IEEE/ACM Transactions on Audio, Speech, and Language Processing 26, no. 10 (2018): 1884-1896.
- Fontana, Federico, and Enrico Bozzo. "Newton-Raphson solution of nonlinear delay-free loop filter networks." IEEE/ACM Transactions on Audio, Speech, and Language Processing 27, no. 10 (2019): 1590-1600.

Credit: Enrico Bozzo

Discrete-Time Simulation of Nonlinear Musical Circuits by means of Physically-Interpretable Iterative Solvers–Part II: Wave Digital Methods

Alberto Bernardini[1] & Federico Fontana[2]

[1]Politecnico di Milano, Italy
`alberto.bernardini@polimi.it`
[2]University of Udine, Italy
`federico.fontana@uniud.it`

6 September 2022

The 25th International Conference on Digital Audio Effects

Outline

Outline

Circuital Models of Audio Systems

- The model of an electrical circuit is made of
  - Equations describing the network topology called:
    - *Kirchhoff Voltage Laws* (KVL)
    - *Kirchhoff Current Laws* (KCL)
  - Constitutive equations of circuit elements such as:
    - *One-port elements* (e.g., sources, resistors, capacitors, inductors, diodes)
    - *Multi-port elements* (e.g., opamps, transformers, gyrators, transistors, vacuum tubes)
- When implicit discretization methods are used, the resulting system of discrete-time equations in the Kirchhoff domain is implicit
  - Constitutive equations and topological information are merged

Wave Digital Filters and Circuit Emulation

- Wave Digital Filter (WDF) theory developed by A. Fettweis during the 70s was *originally conceived as a methodology for modeling digital filters by discretizing reference analog circuits*
- WDF theory poses the basis for completely *new methods for emulating linear and nonlinear circuits* in the Wave Digital (WD) domain

Figure: Photo of Alfred Fettweis.

General Considerations on WDFs

- A WDF is derived discretizing a *reference analog circuit*
- Circuit elements and circuit topology are modeled separately
- One-port circuit elements are modeled as *input-output blocks* characterized by scattering relations
- Topological interconnections of elements are modeled using MIMO *junctions* characterized by scattering matrices
- Elements and junctions are modeled in a *port-wise fashion*
- Each port of an element or junction is characterized by a pair of port variables called *wave variables*
- One *free parameter* is introduced for each port

Outline

Definition of Voltage Waves

- Kirchhoff variables at port n (of a generic port element or junction) are
  - the port voltage v_n
  - the port current i_n
- Wave variables (voltage waves) are defined as [1]

$$a_n = v_n + Z_n i_n \qquad b_n = v_n - Z_n i_n \tag{1}$$

  - a_n is the incident wave
  - b_n is the reflected wave
  - $Z_n \neq 0$ is a scalar free parameter called *reference port resistance*
- Inverse mapping

$$v_n = \frac{a_n + b_n}{2} \qquad i_n = \frac{a_n - b_n}{2Z_n} \tag{2}$$

Outline

Constitutive Equations of One-Port Elements

- In the continuous-time domain (t is the time variable)

$$\xi\left(v(t), i(t)\right) = 0 \tag{3}$$

  - $v(t)$ is the port voltage and $i(t)$ is the port current
  - ξ is a (linear or nonlinear) dynamic or instantaneous function

- In the discrete-time domain

$$\widetilde{\xi}\left(v[k], i[k]\right) = 0 \tag{4}$$

  - $v[k] = v(kT_\mathsf{s})$ and $v[k] = v(kT_\mathsf{s})$, where k is the sampling index and $F_\mathsf{s} = 1/T_\mathsf{s}$ is the sampling frequency
  - if the element is memoryless we have that $\widetilde{\xi}(x, y) = \xi(x, y)$, otherwise $\widetilde{\xi}(x, y) \neq \xi(x, y)$

Linear One-Port Elements

- The majority of linear one-port elements in the discrete-time domain is characterized by a *constitutive equation* in the form

$$v[k] = R_{\mathsf{e}}[k]i[k] + V_{\mathsf{e}}[k] \tag{5}$$

  - $R_{\mathsf{e}}[k]$ is a resistance parameter
  - $V_{\mathsf{e}}[k]$ is a voltage bias parameter

Linear Resistor

- In the continuous-time domain the *constitutive equation* of a linear resistor with resistance R is

$$v(t) = Ri(t) \tag{6}$$

- In the discrete-time domain we get

$$v[k] = Ri[k] \tag{7}$$

- Eq. (7) is a special case of eq. (5) in which:
  - $R_{\mathsf{e}}[k] = R$
  - $V_{\mathsf{e}}[k] = 0$

Linear Resistive Voltage Generator

- In the continuous-time domain the *constitutive equation* of a linear resistive voltage source with source signal $V_{\mathrm{g}}(t)$ and internal series resistance R_{g} is

$$v(t) = R_{\mathrm{g}} i(t) + V_{\mathrm{g}}(t) \tag{8}$$

- In the discrete-time domain we get

$$v[k] = R_{\mathrm{g}} i[k] + V_{\mathrm{g}}[k] \tag{9}$$

- Eq. (9) is a special case of eq. (5) in which:
  - $R_{\mathsf{e}}[k] = R_{\mathrm{g}}$
  - $V_{\mathsf{e}}[k] = V_{\mathrm{g}}[k] = V_{\mathrm{g}}(kT_{\mathsf{s}})$

Linear Dynamic Elements

- In the continuous-time domain the *constitutive equation* of a linear dynamic element (capacitor or inductor) is

$$y(t) = \mu \frac{\mathrm{d}x(t)}{\mathrm{d}t} \tag{10}$$

  - $x(t)$ is a port voltage or port current
  - $y(t)$ is a port current or port voltage
  - μ is a (capacitative or inductive) real coefficient

- In the Laplace domain, where s is the complex frequency variable, (10) is written as

$$Y(s) = s\mu X(s) \tag{11}$$

Possible Time Derivative Approximations

Mappings from the Laplace domain with complex frequency variable s to the Z-domain with complex variable $z = e^{sT_\mathsf{s}}$

- Backward Euler Method

$$s \leftarrow \frac{1 - z^{-1}}{T_\mathsf{s}} \tag{12}$$

- Trapezoidal Rule (a.k.a. bilinear transform or Tustin's method)

$$s \leftarrow \frac{2}{T_\mathsf{s}} \frac{1 - z^{-1}}{1 + z^{-1}} \tag{13}$$

- Many other discretization methods are usable (e.g., finite difference methods, Runge-Kutta methods, etc . . .)

Linear Capacitor

- In the Laplace domain the *constitutive equation* of a linear capacitor with capacitance C is

$$I(s) = sCV(s) \tag{14}$$

- After applying the bilinear transform (13) to (14), in the discrete-time domain we get

$$v[k] = \frac{T_\mathsf{s}}{2C} i[k] + \frac{T_\mathsf{s}}{2C} i[k-1] + v[k-1] \tag{15}$$

- Eq. (15) is a special case of eq. (5) in which [2]:
  - $R_\mathsf{e}[k] = T_\mathsf{s}/(2C)$
  - $V_\mathsf{e}[k] = T_\mathsf{s} i[k-1]/(2C) + v[k-1]$

Linear Inductor

- In the Laplace domain the *constitutive equation* of a linear inductor with inductance L is

$$V(s) = sLI(s) \tag{16}$$

- After applying the bilinear transform (13) to (16), in the discrete-time domain we get

$$v[k] = \frac{2L}{T_\mathsf{s}} i[k] + \frac{2L}{T_\mathsf{s}} i[k-1] - v[k-1] \tag{17}$$

- Eq. (17) is a special case of eq. (5) in which [2]:
  - $R_\mathsf{e}[k] = 2L/T_\mathsf{s}$
  - $V_\mathsf{e}[k] = (2Li[k-1])/T_\mathsf{s} - v[k-1]$

Linear Wave Digital One-Port Element

- Kirchhoff-to-Wave transformation in the discrete-time domain

$$v[k] = \frac{a[k] + b[k]}{2} \quad , \qquad i[k] = \frac{a[k] - b[k]}{2Z[k]} \tag{18}$$

- Applying the substitution (18) in (5) and solving for $b[k]$, we get the scattering relation of a generic linear one-port element

$$b[k] = \frac{R_{\mathsf{e}}[k] - Z[k]}{R_{\mathsf{e}}[k] + Z[k]} a[k] + \frac{2Z[k]}{R_{\mathsf{e}}[k] + Z[k]} V_{\mathsf{e}}[k] \tag{19}$$

- Adaptation case (the instantaneous dependency of $b[k]$ from $a[k]$ is eliminated)

$$b[k] = V_{\mathsf{e}}[k] \quad , \qquad \text{with} \qquad Z[k] = R_{\mathsf{e}}[k] \tag{20}$$

Implementation of Linear WD One-Ports

Table: *Wave mappings of common WD linear one-port elements.*

Constitutive Eq.	Wave Mapping	Adaptation Condition
$v(t) = V_{\mathrm{g}}(t) + R_{\mathrm{g}} i(t)$	$b[k] = V_{\mathrm{g}}[k]$	$Z[k] = R_{\mathrm{g}}$
$v(t) = Ri(t)$	$b[k] = 0$	$Z[k] = R$
$i(t) = C\dfrac{dv(t)}{dt}$	$b[k] = a[k-1]$	$Z[k] = \dfrac{T_{\mathrm{s}}}{2C}$
$v(t) = L\dfrac{di(t)}{dt}$	$b[k] = -a[k-1]$	$Z[k] = \dfrac{2L}{T_{\mathrm{s}}}$

Nonlinear Diode Model with Resistances

- Extended Shockley diode model for exponential p–n junction diodes

$$\xi(v,i) = Is\left(e^{\frac{v-R_s i}{\eta V_t}} - 1\right) + \frac{v - R_s i}{R_p} - i = 0, \qquad (21)$$

  - saturation current I_{s}
  - thermal voltage V_{th}
  - ideality factor η
  - series resistance R_s
  - parallel resistance R_p
- Eq. (21) is nonlinear and it cannot be put in the form (5)

Nonlinear WD Diode Model

- Substitute (18) into the discrete-time version of eq. (21)
- The result is a *transcendental equation* in the WD domain
- The following closed-form solution for b can be found [3, 4]

$$b = f(a) = -\frac{\omega\left(\lambda - \sigma\frac{\mu}{\kappa} + \ln\left(-\frac{\sigma}{\kappa}\right)\right)}{\sigma} - \frac{\mu}{\kappa}, \qquad (22)$$

$$\begin{aligned} \sigma &= \frac{Z^{1-\rho} + R_s Z^{-\rho}}{2\eta V_t}, \quad \lambda = \frac{a\left(Z^{1-\rho} - R_s Z^{-\rho}\right)}{2\eta V_t}, \\ \kappa &= -\frac{Z^{1-\rho} + Z^{-\rho}(R_s + R_p)}{2 I_s R_p}, \\ \mu &= 1 - \frac{a\left(Z^{1-\rho} - Z^{-\rho}(R_s + R_p)\right)}{2 I_s R_p}. \end{aligned} \qquad (23)$$

  - ω is the Omega Wright function, defined in terms of the first branch of the Lambert function as $\omega(x) = \mathcal{W}_0(e^x)$ with $x \in \mathbb{R}$
- The nonlinear WD diode cannot be adapted!

Thèvenin Equivalent of Nonlinear One-Ports

- If we consider a generic operating point (v_0, i_0) on the nonlinear v-i curve, we can locally approximate the nonlinear element through the linearization

$$v = R_{\mathsf{e}}(v_0, i_0)i + V_{\mathsf{e}}(v_0, i_0) \tag{24}$$

- (24) is a line with slope R_{e} and y-intercept V_{e} that is tangent to the v-i curve and passes through (v_0, i_0).
- For the extended Shockley model, we can write

$$R_{\mathsf{e}}(v,i) = v'(i) = -\frac{\partial\xi(v,i)/\partial i}{\partial\xi(v,i)/\partial v} = \frac{1 + \frac{R_s}{R_p} + \frac{I_s R_s}{\eta V_t} e^{\frac{v - R_s i}{\eta V_t}}}{\frac{1}{R_p} + \frac{I_s}{\eta V_t} e^{\frac{v - R_s i}{\eta V_t}}}. \tag{25}$$

$$V_{\mathsf{e}}(v,i) = v - R_{\mathsf{e}}(v,i)i \tag{26}$$

Thèvenin Equivalent of Nonlinear One-Ports

- The local Thèvenin equivalent model that approximates the nonlinearity close to the operating point (v_0, i_0) could thus be adapted by setting

$$Z = R_\mathsf{e}(v_0, i_0) \tag{27}$$

- However, in most scenarios, knowing (v_0, i_0) requires to already have the circuit solution at disposal!
- $R_\mathsf{e}(v_0, i_0)$ needs to be estimated exploiting the past samples of the simulation

Outline

Topological Junctions or Connection Networks

- A N-port topological junction is an open interconnection network (i.e., without *electrical loads*) characterized by
  - a vector of port voltages $\mathbf{v} = [v_1, \dots, v_N]^T$
  - a vector of port currents $\mathbf{i} = [i_1, \dots, i_N]^T$
- Example:

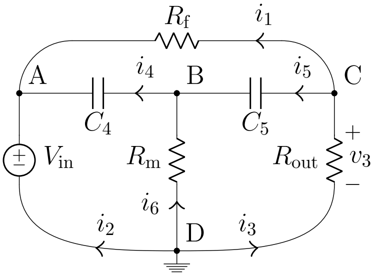

(a) Reference circuit.

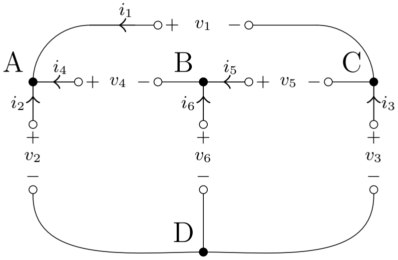

(b) Topological connection network.

Relations between Port Variables

- Found a *subset of independent port voltages* we have that

$$\mathbf{v} = \mathbf{Q}^T \mathbf{v}_{\mathsf{t}} \tag{28}$$

  - $\mathbf{v}_{\mathsf{t}}$ is the vector of size $q \times 1$ collecting independent port voltages
  - $\mathbf{Q}$ is the fundamental cut-set matrix of size $q \times N$
- Found a *subset of independent port currents* we have that

$$\mathbf{i} = \mathbf{B}^T \mathbf{i}_{\mathsf{l}} \tag{29}$$

  - $\mathbf{i}_{\mathsf{l}}$ is the vector of size $p \times 1$ collecting independent port currents
  - $\mathbf{B}$ is the fundamental loop matrix of size $p \times N$
- $p + q = N$
- Orthogonality property

$$\mathbf{B}\mathbf{Q}^T = \mathbf{0}_{p\times q} \quad , \qquad \mathbf{Q}\mathbf{B}^T = \mathbf{0}_{q\times p} \tag{30}$$

How to find independent port variables?

- Consider the digraph $\mathcal{D}$ of the reference circuit where the *edges* represent the loads of the connection network (one per port), while the *vertices* represent the nodes of the circuit [5]
- Apply a tree-cotree decomposition to $\mathcal{D}$
  - A tree $\mathcal{T}$ of $\mathcal{D}$ is defined as *a connected acyclic subgraph of $\mathcal{D}$ containing all vertices*
  - A cotree $\mathcal{C}$ of $\mathcal{D}$ is *a subgraph of $\mathcal{D}$ containing all the edges of $\mathcal{D}$ that are not in a reference tree $\mathcal{T}$*
- Independent port voltages in $\mathbf{v}_{\mathrm{t}}$ are those *related to the edges of the tree*
- Independent port currents in $\mathbf{i}_{\mathrm{l}}$ are those *related to the edges of the cotree*

Example 1: Series Connection Network

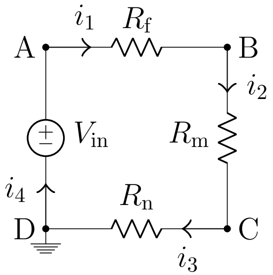

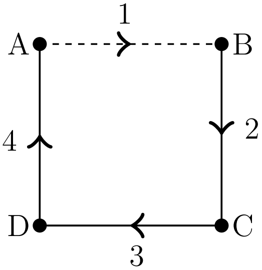

$$\mathbf{i} = \mathbf{B}^T \mathbf{i}_\mathsf{l} \quad \rightarrow \quad \begin{bmatrix} i_1 \\ i_2 \\ i_3 \\ i_4 \end{bmatrix} = \begin{bmatrix} 1 \\ 1 \\ 1 \\ 1 \end{bmatrix} i_1 \tag{31}$$

Example 2: Parallel Connection Network

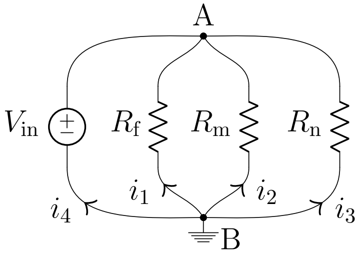

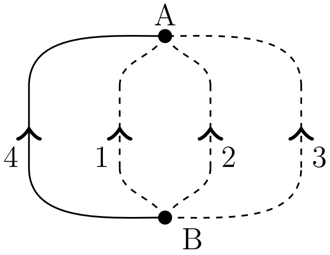

$$\mathbf{v} = \mathbf{Q}^T \mathbf{v}_{\mathsf{t}} \quad \rightarrow \quad \begin{bmatrix} v_1 \\ v_2 \\ v_3 \\ v_4 \end{bmatrix} = \begin{bmatrix} 1 \\ 1 \\ 1 \\ 1 \end{bmatrix} v_4 \tag{32}$$

Example 3: Bridged-Tee Connection Network

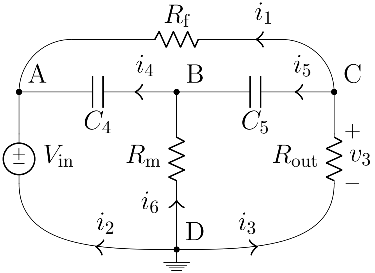

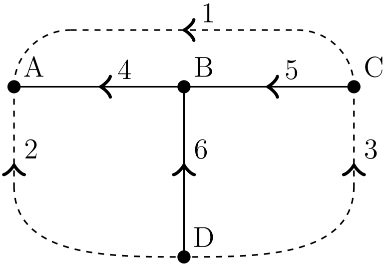

$$\mathbf{i} = \mathbf{B}^T \mathbf{i}_\mathrm{l} \quad \rightarrow \quad \begin{bmatrix} i_1 \\ i_2 \\ i_3 \\ i_4 \\ i_5 \\ i_6 \end{bmatrix} = \begin{bmatrix} 1 & 0 & 0 \\ 0 & 1 & 0 \\ 0 & 0 & 1 \\ -1 & -1 & 0 \\ -1 & 0 & 1 \\ 0 & -1 & -1 \end{bmatrix} \begin{bmatrix} i_1 \\ i_2 \\ i_3 \end{bmatrix} \tag{33}$$

WD Junctions (Adaptors)

- In the WD domain a topological connection network is modeled as a WD scattering junction (also called *adaptor*)
- Kirchhoff-to-Wave mapping of port variables

$$\mathbf{v} = \frac{1}{2}(\mathbf{a} + \mathbf{b}) \quad , \quad \mathbf{i} = \frac{1}{2}\mathbf{Z}^{-1}(\mathbf{b} - \mathbf{a}) \tag{34}$$

  - $\mathbf{a} = [a_1, \dots, a_N]^T$ vector of waves reflected by the junction
  - $\mathbf{b} = [b_1, \dots, b_N]^T$ vector of waves incident to the junction
  - $\mathbf{Z} = \mathrm{diag}[Z_1, \dots, Z_N]$ is the diagonal matrix of free parameters
- Scattering relation

$$\mathbf{a} = \mathbf{S}\mathbf{b} \tag{35}$$

  - $\mathbf{S}$ is a $N \times N$ scattering matrix

Formation of the Scattering Matrix

- If $q \leq p$ use

$$\mathbf{S} = 2\mathbf{Q}^T(\mathbf{Q}\mathbf{Z}^{-1}\mathbf{Q}^T)^{-1}\mathbf{Q}\mathbf{Z}^{-1} - \mathbf{I} \qquad (36)$$

  - $\mathbf{I}$ is the $N \times N$ identity matrix
  - the inversion of the $q \times q$ matrix $\mathbf{Q}\mathbf{Z}^{-1}\mathbf{Q}^T$ is required

- If $q \geq p$

$$\mathbf{S} = \mathbf{I} - 2\mathbf{Z}\mathbf{B}^T(\mathbf{B}\mathbf{Z}\mathbf{B}^T)^{-1}\mathbf{B} \qquad (37)$$

  - $\mathbf{I}$ is the $N \times N$ identity matrix
  - the inversion of the $p \times p$ matrix $\mathbf{B}\mathbf{Z}\mathbf{B}^T$ is required

Properties of the Scattering Matrix

- Losslessness:

$$\mathbf{S}^T\mathbf{Z}^{-1}\mathbf{S} = \mathbf{Z}^{-1} \tag{38}$$

- Self-inverse Property:

$$\mathbf{S}\mathbf{S} = \mathbf{I} \tag{39}$$

- Reciprocity:

$$\mathbf{S}^T\mathbf{Z}^{-1} = \mathbf{Z}^{-1}\mathbf{S} \tag{40}$$

Reflection-Free Ports in WD Junctions

- One port of a topological WD junction can be made reflection-free (we say *the port is adapted*)
- The nth port of a WD junction is made reflection-free if the nth diagonal entry s_{nn} of $\mathbf{S}$ is imposed to be zero

$$s_{nn} = 0 \tag{41}$$

- Condition (41) can be satisfied by properly setting the free parameter Z_n
- Examples
  - The nth port of a N-port series WD junction is made reflection-free by setting $Z_n = \sum_{k \neq n} Z_k$
  - The nth port of a N-port parallel WD junction is made reflection-free by setting $Z_n^{-1} = \sum_{k \neq n} Z_k^{-1}$

Outline

Modeling WDF Structures with One Nonlinearity

- The WDF is modeled as a connection tree
- *The nonlinear one-port element* is the root
- *WD topological junctions* are the nodes
  - *Ports of WD junctions either connected to other WD junctions or to the nonlinear element are made reflection-free*
- *Linear WD one-port elements* are the leaves
  - *Linear WD elements are all adapted*
- In case the topology is solely made of *series-parallel connections*, the WDF can be modeled as a Binary Connection Tree (BCT)
  - In a BCT nodes are 3-port series or parallel WD junctions [6]

Generic Connection Tree with One Node

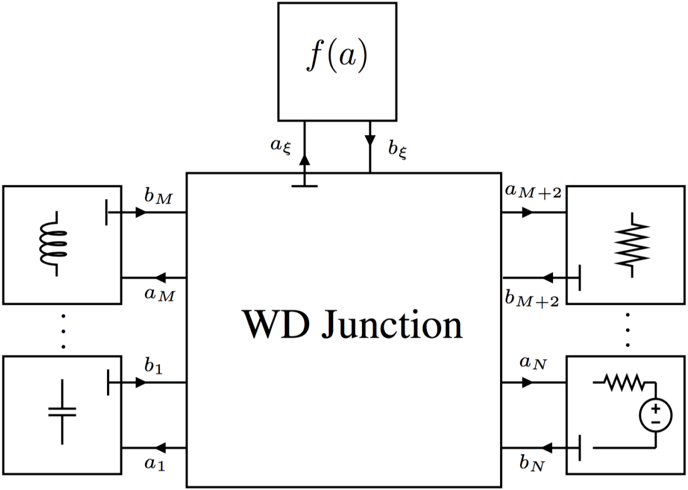

Example of Binary Connection Tree

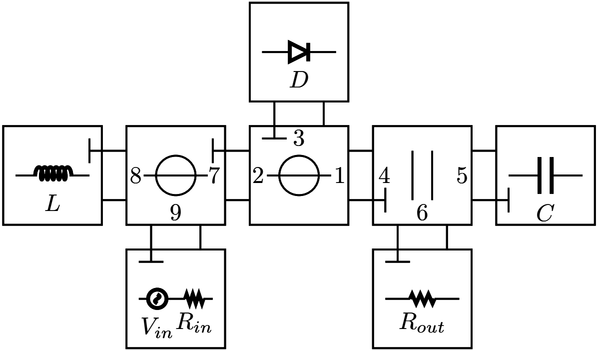

- In the BCT structure nodes are 3-port series/parallel adaptors.

Outline

Introduction

Definition of Wave Variables

Modeling the Elements

Modeling the Topology

WDFs with One Nonlinearity

WDFs with Multiple Nonlinearities
- Scattering Iterative Method (SIM)
- Wave Digital Newton-Raphson (WDNR)

Brief Overview on Iterative WD Methods (1/2)

Fixed-point methods:

- In **Schwerdtfeger et al.** [7, 8] a fixed-point method invoking the multi-dimensional WDF formalism [9] was developed.
- Another WD fixed-point method was proposed in [10] by **Kabir et al.** who discussing the future works noticed that: "*the optimum selection of reference impedances* (port resistances) *at nonlinear device ports [. . .] may have to be adaptive since the optimum values are dependent on the circuit state.*"
- **Scattering Iterative Method (SIM)** (*described later*). There were no systematic studies on the optimal selection of reference port resistances until the publication of SIM by **Bernardini et al.**, originally proposed in [11, 12] for the analysis of large nonlinear photovoltaic arrays and later extended in [13, 2, 14, 15] for the solution of dynamic nonlinear audio circuits.

Brief Overview on Iterative WD Methods (2/2)

Newton Raphson methods or variants thereof:

- **Christoffersen** proposed in [16] a hybrid scheme including fixed-point and NR method as particular cases, showing flexibility and efficiency in solving several nonlinear circuits.
- Other Newton's approximated schemes using the secant method applied to a diode clipper circuit were discussed in **Schwerdtfeger et al.** [17].
- An NR method based on automatic differentiation is applied by **Kolonko et al.** in [18] for solving the circuit in [17].
- Further NR methods using backtracking and improved initial guesses proved to fit WD models of a diode clipper circuit and a circuit with a 2-port transistor in **Olsen et al.** [19].
- NR method proposed by **Bernardini et al.** [20] (*described later*).

Outline

- Introduction
- Definition of Wave Variables
- Modeling the Elements
- Modeling the Topology
- WDFs with One Nonlinearity
- WDFs with Multiple Nonlinearities
  - Scattering Iterative Method (SIM)
  - Wave Digital Newton-Raphson (WDNR)

Scattering Iterative Method (SIM): WDF Structure

Let us consider a WDF structure composed of:

- an arbitrary reciprocal lossless scattering junction characterized by scattering matrix $\mathbf{S}$
- (non)linear one-port elements connected to the junction
- $\mathbf{a} = [a_1, \dots, a_N]^T$, i.e., the vector of waves incident to the elements and reflected from the junction
- $\mathbf{b} = [b_1, \dots, b_N]^T$, i.e., the vector of waves incident to the junction and reflected from the elements
- $\mathbf{Z} = \mathrm{diag}([Z_1, \dots, Z_N])$, i.e., the matrix of port resistances

SIM: Example of WDF Structure

Ring modulator circuit and its WDF realization:

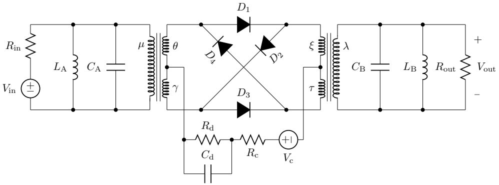

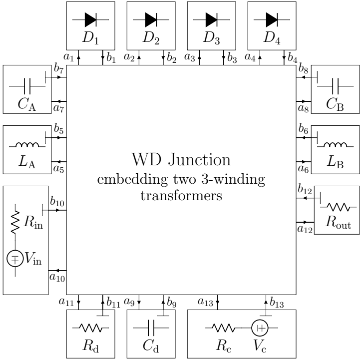

SIM Stages

SIM is a fixed-point iterative method that solves the reference circuit at each sampling step k by performing the stages:

- Initialization
- Local Scattering Stage
- Global Scattering Stage
- Convergence Check

SIM: Initialization

- At a given sampling step k, the diagonal matrix $\mathbf{Z}[k]$ of free parameters is firstly updated.
  - Free parameters Z_n corresponding to linear elements are set according to the adaptation conditions.
  - **Free parameters** Z_n of nonlinear elements are set **as close as possible to the slopes of the tangent lines passing through the operating points on the** v–i **characteristics**.
  - Since the operating points at sampling step k are not known at this stage, as an estimate, we set the free parameters equal to the tangent slopes at sampling step $k-1$.
- Then, the updated $\mathbf{Z}[k]$ is also used to update the scattering matrix $\mathbf{S}[k]$.
- The vector of waves incident to the elements is initialized as $\mathbf{a}^{(0)}[k] = \mathbf{a}[k-1]$.

SIM: Local Scattering Stage

The waves reflected from the elements and incident to the junction are computed.

- For **linear elements**, the reflected waves are computed explicitly according to the scattering relations in Table 1, and remain fixed during SIM iterations until convergence:

$$b_n^{(\gamma)}[k] = V_{\mathsf{en}}[k] \ . \tag{42}$$

- For **nonlinear elements**, at each SIM iteration γ we compute:

$$b_n^{(\gamma)}[k] = f_n(a_n^{(\gamma-1)}[k]) \ . \tag{43}$$

SIM: Global Scattering Stage

At each SIM iteration γ, the waves incident to the elements are computed as

$$\mathbf{a}^{(\gamma)}[k] = \mathbf{S}[k]\mathbf{b}^{(\gamma)}[k] \tag{44}$$

SIM: Convergence Check

- Local and global scattering stages are repeated until the following convergence condition is met

$$||\mathbf{v}^{(\gamma)}[k] - \mathbf{v}^{(\gamma-1)}[k]|| < \epsilon_{\mathsf{SIM}} \tag{45}$$

  is met, where

$$\mathbf{v}^{(\gamma)}[k] = \frac{1}{2}\left(\mathbf{a}^{(\gamma)}[k] + \mathbf{b}^{(\gamma)}[k]\right)$$

- The tolerance ϵ_{SIM} is a small number, e.g. $\epsilon_{\mathsf{SIM}} = 10^{-4}$.

SIM Convergence Analysis

- Let us rewrite the *Global Scattering Stage* (omitting $[k]$ for the sake of readability)

$$\mathbf{a}^{(\gamma)} = \mathbf{S}\mathbf{b}^{(\gamma)} \tag{46}$$

- Making also the *Local Scattering Stage* explicit, we get

$$\mathbf{a}^{(\gamma)} = \mathbf{S}\mathbf{f}\left(\mathbf{a}^{(\gamma-1)}\right) \tag{47}$$

where

$$\mathbf{f}(\mathbf{a}) = \left[f_1(a_1), \ldots, f_N(a_N)\right]^T .$$

SIM Convergence Analysis

- The fixed-point iterative process of SIM is characterized by the repeated application of the vector function

$$\mathbf{h}(\mathbf{a}) \doteq \mathbf{S}\mathbf{f}(\mathbf{a}). \tag{48}$$

- Recalling the Banach Fixed-Point Theorem [21]; having a *contractive mapping* $\mathbf{h} : \Omega \subset \mathbb{R}^N \to \mathbb{R}^N$ with $\mathbf{a} \in \Omega$,

$$\mathbf{a}^{(\gamma)} = \mathbf{h}(\mathbf{a}^{(\gamma-1)}) \tag{49}$$

  has a fixed-point $\mathbf{a}^*$ (i.e., $\mathbf{a}^* = \mathbf{h}(\mathbf{a}^*)$), and a sequence of iterates $\mathbf{a}^{(\gamma)}$ converges to $\mathbf{a}^*$.
- To guarantee the SIM convergence it is sufficient to prove the mapping $\mathbf{h}(\mathbf{a})$ to be contractive.

SIM Convergence Analysis

- According to the mean value theorem for vector-valued functions [22], any functional map having its Jacobian norm less than one is a contraction.
- Defined the Jacobian matrix of $\mathbf{h}(\mathbf{a})$ as $\mathbf{J_h}(\mathbf{a})$, we can conveniently verify this condition using the *spectral radius* of $\mathbf{J_h}(\mathbf{a})$, since for every matrix norm $||.||$ we have that

$$\rho(\mathbf{J_h}(\mathbf{a})) \leq ||\mathbf{J_h}(\mathbf{a})|| \tag{50}$$

- Therefore, the condition

$$\rho(\mathbf{J_h}(\mathbf{a})) < 1 \tag{51}$$

is sufficient for $\mathbf{h}(\mathbf{a})$ to be a contraction.

SIM Convergence Analysis

- The Jacobian of $\mathbf{h}(\mathbf{a})$ can be expressed as

$$\mathbf{J_h}(\mathbf{a}) = \mathbf{S}\mathbf{J_f}(\mathbf{a}) \tag{52}$$

  where $\mathbf{J_f}(\mathbf{a})$ is the Jacobian of $\mathbf{f}(\mathbf{a})$ and is given by

$$\mathbf{J_f}(\mathbf{a}) = \mathrm{diag}\left([f_1'(a_1), \ldots, f_N'(a_N)]\right) \tag{53}$$

  where $f_n'(a_n)$ is the derivative of the nth WD element scattering relation w.r.t. a_n.
- The SIM convergence condition can hence be rewritten as

$$\rho\left(\mathbf{S}\mathbf{J_f}(\mathbf{a})\right) < 1\,. \tag{54}$$

SIM Convergence Analysis

It can be proven that if

1. the topological junction is lossless and reciprocal

$$\mathbf{S}^T\mathbf{Z}^{-1}\mathbf{S} = \mathbf{Z}^{-1}\ , \quad \mathbf{SS} = \mathbf{I} \tag{55}$$

2. one-ports are characterized by strictly monotonically increasing v–i characteristics

$$v_n'(i_n) > 0 \tag{56}$$

then SIM globally (always) converges to the fixed point!

SIM Convergence Analysis

- It can be proven that if the topological junction is lossless and reciprocal and $\mathbf{J_f}(\mathbf{a})$ is diagonal (only one-port elements)

$$\rho\left(\mathbf{S}\mathbf{J_f}(\mathbf{a})\right) \leq \rho\left(\mathbf{J_f}(\mathbf{a})\right) \tag{57}$$

- $\rho\left(\mathbf{J_f}(\mathbf{a})\right)$ is the largest diagonal entry of $\mathbf{J_f}(\mathbf{a})$ in modulus!

SIM Convergence Analysis

- Let us define waves as functions of current i

$$\begin{aligned} a &= v(i) + Zi = \phi(i) \\ b &= v(i) - Zi = \psi(i) = \psi(\phi^{-1}(a)) \end{aligned}$$

- We can express the nth diagonal entry of $\mathbf{J_f}(\mathbf{a})$ as

$$f_n'(a_n) = \frac{\psi'(\phi^{-1}(a_n))}{\phi'(\phi^{-1}(a_n))} = \frac{v_n'(i_n) - Z_n}{v_n'(i_n) + Z_n} \tag{58}$$

where $f_n'(a_n)$ is the derivative of $f_n(a_n)$ w.r.t. a_n, whereas $v_n'(i_n)$ is the derivative of $v_n(i_n)$ w.r.t. i_n.

- $f_n'(a_n)$ can be thought of as the reflection coefficient of the Thévenin equivalent model.
- Hence, for adapted linear elements we have $f_n'(a_n) = 0$.

SIM Convergence Analysis

- Moreover, according to (58), if we choose the free parameters to be positive, i.e.,
$$Z_n > 0\,, \tag{59}$$
we have that
$$0 \leq |f'_n(a_n)| < 1 \tag{60}$$
because, by assumption, $v'_n(i_n) > 0$.
- Therefore, we can state that convergence is guaranteed since
$$\rho\left(\mathbf{S}\mathbf{J}_{\mathbf{f}}(\mathbf{a})\right) \leq \rho\left(\mathbf{J}_{\mathbf{f}}(\mathbf{a})\right) < 1\,. \tag{61}$$
- Moreover, the lower $\rho\left(\mathbf{J}_{\mathbf{f}}(\mathbf{a})\right)$ the higher the SIM convergence speed!
- It follows that the closer Z_n to $v'_n(i_n)$ the higher the SIM convergence speed!

SIM Properties

- Physically interpretable free parameter choice
  $Z_n = R_{\mathsf{e}n} = v_n'(i_n)$
- Guarantee of Convergence for circuits with one-port monotonically increasing nonlinearities and reciprocal lossless junctions
- Accuracy
- Efficiency
- Parallelizability: the *Local Scattering Stage* is *embarrassingly parallelizable*
- Accommodation of time-varying parameters at no additional cost!

Bottleneck of SIM

- *Initialization Stage* is the bottleneck of SIM: in particular, **the update of S at every sample**
- Keeping $Z_n \approx R_{\mathsf{e}n}$ has the advantage of maintaining the spectral radius of the SIM iteration matrix small
- However the advantage gained in updating the free parameters Z_n is counterbalanced by the cost of recomputing the scattering matrix $\mathbf{S}$

Dynamic Scattering Matrix Recomputation (DSR)

Let us define the metric

$$\phi[k-1] = \sum_{n=1}^{N} |R_{\mathsf{e}n}(v_n[k-1], i_n[k-1]) - Z_n[k-1]|$$

- given a small threshold ξ_{DSR}
- if $\phi[k-1] \leq \xi_{\mathsf{DSR}} \rightarrow Z_n$ and $\mathbf{S}$ are left unaltered
- if $\phi[k-1] > \xi_{\mathsf{DSR}} \rightarrow Z_n$ and $\mathbf{S}$ are updated

DSR Example: Asymmetric Diode Clipper

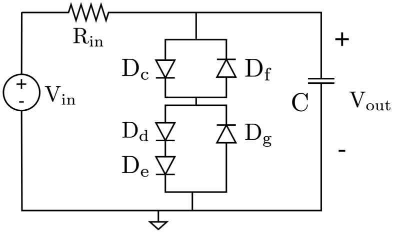

(i) Circuit

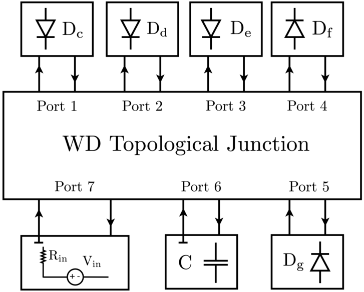

(j) WDF

DSR Example: Asymmetric Diode Clipper

TABLE I
PERFORMANCE COMPARISON BETWEEN STD-SIM AND DSR-SIM

	STD-SIM	DSR-SIM
RTR	1.43	0.89
Avg. Numb. of Iterations per Sample	1.48	1.60
Avg. Iteration Time per Sample	2.25 μs	2.40 μs
Avg. Z, S Update Time per Sample	5.88 μs	2.66 μs
Avg. Total Time per Sample	8.13 μs	5.06 μs

TABLE II
PERCENTAGES OF EXECUTION TIME IN STD-SIM AND DSR-SIM

	STD-SIM	DSR-SIM
Iteration Time	27.7 %	47.4 %
Z, S Update Time	72.3 %	52.6 %

DSR Example: Asymmetric Diode Clipper

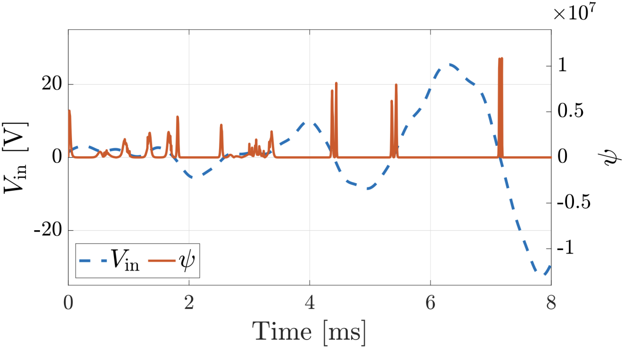

Outline

WDNR: Definition of the Iteration Function

- Let us define the function $\mathbf{g}(\mathbf{a}) = [g_1(\mathbf{a}), \ldots, g_N(\mathbf{a})]^T$ as

$$\mathbf{g}(\mathbf{a}) = \mathbf{S}\mathbf{a} - \mathbf{f}(\mathbf{a}) \ , \tag{62}$$

such that at the fixed-point $\mathbf{a}^*$ we have

$$\mathbf{g}(\mathbf{a}^*) = \mathbf{S}\mathbf{a}^* - \mathbf{f}(\mathbf{a}^*) = \mathbf{0} \ . \tag{63}$$

- Its Jacobian matrix is

$$\mathbf{J}_{\mathbf{g}}(\mathbf{a}) = \mathbf{S} - \mathbf{J}_{\mathbf{f}}(\mathbf{a}) \ , \tag{64}$$

where

$$\mathbf{J}_{\mathbf{f}}(\mathbf{a}) = \operatorname{diag}\left[f_1'(a_1), \ldots, f_N'(a_N)\right] \ . \tag{65}$$

WDNR Method

- Set the initial guess $\mathbf{a}^{(0)}$, we apply the NR iterative update rule

$$\mathbf{a}^{(\gamma)} = \mathbf{a}^{(\gamma-1)} - \mathbf{J}_{\mathbf{g}}^{-1}\left(\mathbf{a}^{(\gamma-1)}\right)\mathbf{g}\left(\mathbf{a}^{(\gamma-1)}\right) \quad . \tag{66}$$

- Defined a small tolerance ξ_{WDNR}, the stop condition is

$$\left\|\mathbf{v}^{(\gamma)} - \mathbf{v}^{(\gamma-1)}\right\| < \xi_{\mathsf{WDNR}} \ , \tag{67}$$

  where

$$\mathbf{v}^{(\gamma)} = \frac{1}{2}\left(\mathbf{a}^{(\gamma)} + \mathbf{f}\left(\mathbf{a}^{(\gamma)}\right)\right) \quad .$$

- the above operations are done at each sampling step k

WDNR Quadratic Convergence Conditions

- There exists a *basin* around the **solution** $\mathbf{a}$ where the NR solver can be initialized to converge on $\mathbf{a}$ with quadratic speed.
- The *basin* is included inside an hypersphere centered on the solution point $\mathbf{a}$ and with radius $1/M(\mathbf{a})$ such that

$$M(\mathbf{a}) = \frac{1}{2}\left\|\mathbf{J}_{\mathbf{g}}^{-1}(\mathbf{a})\mathbf{H}_{\mathbf{g}}(\mathbf{a})\right\|_{\infty} \leq \frac{\sqrt{N}}{2}\left\|\mathbf{J}_{\mathbf{g}}^{-1}(\mathbf{a})\mathbf{H}_{\mathbf{g}}(\mathbf{a})\right\| \quad (68)$$

where the second order derivatives $f_n''(a_n)$ are collected in

$$\mathbf{H}_{\mathbf{g}}(\mathbf{a}) = -\mathrm{diag}\left[f_1''(a_1), \ldots, f_N''(a_N)\right].$$

- The larger the radius $1/M(\mathbf{a})$, the larger the basin of quadratic convergence

WDNR Quadratic Convergence Conditions

- It can be proven that

$$\left\|\mathbf{J}_{\mathbf{g}}^{-1}(\mathbf{a})\right\| \leq \sqrt{\frac{Z_{\mathsf{max}}}{Z_{\mathsf{min}}}}\frac{1}{1-\left\|\mathbf{J}_{\mathbf{f}}(\mathbf{a})\right\|}, \qquad (69)$$

  in which $\left\|\mathbf{J}_{\mathbf{f}}(\mathbf{a})\right\| < 1$, while Z_{max} and Z_{min} are respectively the largest and smallest port resistance.

- Hence

$$M(\mathbf{a}) \leq \frac{\sqrt{N}}{2}\sqrt{\frac{Z_{\mathsf{max}}}{Z_{\mathsf{min}}}}\frac{\left\|\mathbf{H}_{\mathbf{g}}(\mathbf{a})\right\|}{1-\left\|\mathbf{J}_{\mathbf{f}}(\mathbf{a})\right\|}. \qquad (70)$$

WDNR: Choice of Free Parameters

- How to choose the free parameters (port resistances) Z_n?
- The larger the radius $1/M(\mathbf{a})$, the larger the basin of quadratic convergence
- $$M(\mathbf{a}) \leq \frac{\sqrt{N}}{2}\sqrt{\frac{Z_{\text{max}}}{Z_{\text{min}}}}\frac{\left\|\mathbf{H}_{\mathbf{g}}(\mathbf{a})\right\|}{1-\left\|\mathbf{J}_{\mathbf{f}}(\mathbf{a})\right\|}. \tag{71}$$
  We can **minimize the upper bound** in (71) by both minimizing its numerator and maximizing its denominator.
- Maximizing the denominator is straightforward. In fact, $\left\|\mathbf{J}_{\mathbf{f}}(\mathbf{a})\right\|$ can be set to zero by choosing
  $$Z_n = v_n'(i_n)\ . \tag{72}$$
- The upper bound depends also on the second-order derivatives $f_n''(a_n)$, through $\left\|\mathbf{H}_{\mathbf{g}}(\mathbf{a})\right\|$.

WDNR Quadratic Convergence Conditions

- There is no theoretical guarantee that condition $Z_n = v'_n(i_n)$ minimizes (71). For this reason, this choice remains heuristic.
- $Z_n = v'_n(i_n)$ is attractive since it generalizes the concept of linear one-port adaptation of traditional WDF theory [1].
- In fact, for linear one-ports, the adaptation condition is

$$Z_n = R_{\mathsf{e}n} = v'_n(i_n)$$

- For linear one-ports condition $f''_n(a_n) = 0$ always holds, implying that the radius $1/M(\mathbf{a})$ is infinitely large in a fully linear WD network.
- If all one-ports are linear and condition $Z_n = v'_n(i_n)$ is applied then NR converges in just one iteration.

WDNR Quadratic Convergence Conditions

- There is no quantitative expression putting the size of the basin in relation with the speed of convergence.
- However, there is ample evidence that the larger the basin, the faster the convergence is.
- Notice that condition $Z_n = v'_n(i_n)$ can not be set exactly, as all v_n and i_n variables become apparent *after* the computation through NR of the vector $\mathbf{a}$ of incident waves.
- Keeping robustness and efficiency in mind, a reasonable estimation of the values $v'_n(i_n)$ can be made using the port variables at the previous sampling steps when setting the current port resistances.

WDNR: Ring Modulator Simulations

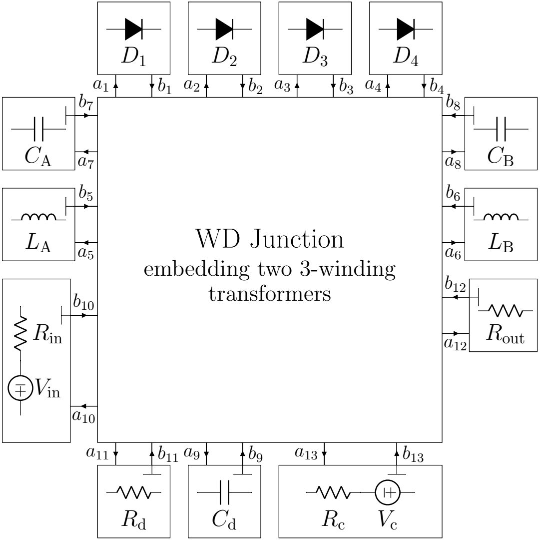

WDNR: Ring Modulator Simulations

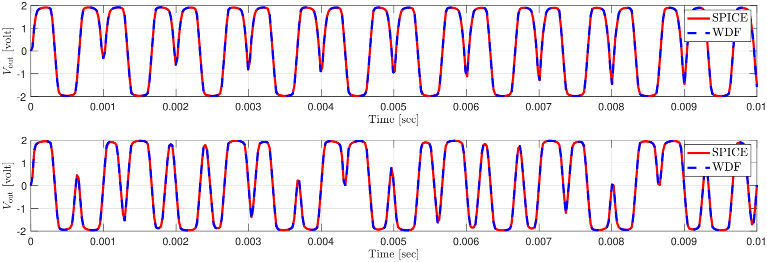

- **Upper plot**: $g_{\mathsf{in}} = 5$ V, $f_{\mathsf{in}} = 1500$ Hz, $g_{\mathsf{c}} = 5$ V and $f_{\mathsf{c}} = 500$ Hz, $F_{\mathsf{s}} = 44.1$ kHz
- **Lower plot**: $g_{\mathsf{in}} = 5$ V, $f_{\mathsf{in}} = 1500$ Hz, $g_{\mathsf{c}} = 5$ V and $f_{\mathsf{c}} = 810$ Hz, $F_{\mathsf{s}} = 44.1$ kHz

WDNR: Ring Modulator Simulations

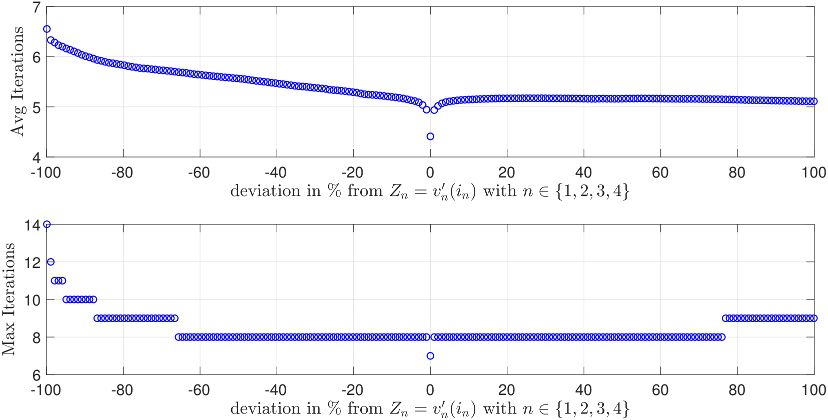

- $g_{\mathsf{in}} = 5$ V, $f_{\mathsf{in}} = 1500$ Hz, $g_{\mathsf{c}} = 5$ V and $f_{\mathsf{c}} = 500$ Hz, $F_{\mathsf{s}} = 44.1$ kHz

WDNR: Ring Modulator Simulations

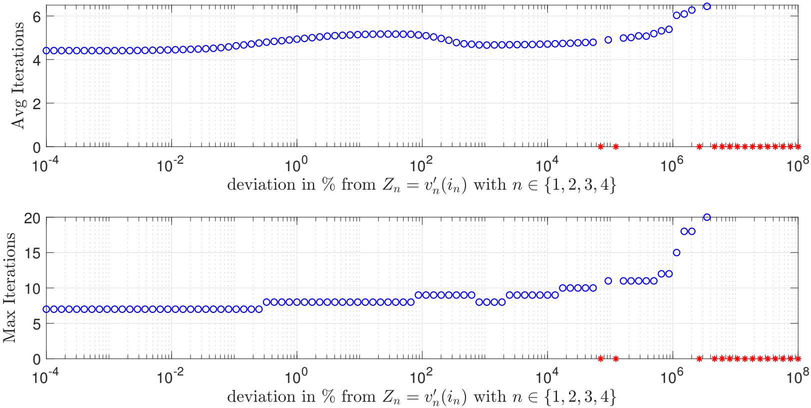

- $g_{\text{in}} = 5$ V, $f_{\text{in}} = 1500$ Hz, $g_{\text{c}} = 5$ V and $f_{\text{c}} = 500$ Hz, $F_{\text{s}} = 44.1$ kHz

Outline

Family of WD Geometric Fixed Point Solvers

A new family of WD solvers is under study!

- The family includes *fixed-point (SIM)* and Newton-Raphson as limit cases
- The *speed of convergence* is higher than fixed-point (linear) and lower than Newton-Raphson (quadratic)
- Except for WDNR, no need to compute inverse Jacobian matrices
- The choice of free parameters $Z_n \approx v'_n(i_n)$ is always *good* for all solvers of the family

A. Bernardini, E. Bozzo, F. Fontana. Wave Digital Geometric Fixed-Point Solvers for Circuits with Multiple One-Port Nonlinearities. To be submitted to Elsevier Signal Processing.

Selected References

SIM for Simulation of Photovoltaic Arrays:

- *A. Bernardini, P. Maffezzoni, L. Daniel, A. Sarti. Wave-based analysis of large nonlinear photovoltaic arrays. IEEE Trans. Circuits Syst. I: Reg. Papers, 65(4):1363–1376, April 2018.*
- *A. Bernardini, A. Sarti, P. Maffezzoni, L. Daniel. Wave digital-based variability analysis of electrical mismatch in photovoltaic arrays. In Proc. IEEE Int. Symp. Circuits Syst. (ISCAS), May 2018.*

Selected References

SIM for Time-Domain Audio Circuit Simulation:

- *A. Bernardini, K. J. Werner, P. Maffezzoni, A. Sarti. Wave digital modeling of the diode-based ring modulator. In Proc. 144th Audio Eng. Soc. Conv., Milan, Italy, May 24–26 2018. conv. paper #10015.*
- *A. Bernardini, P. Maffezzoni, A. Sarti. Linear multistep discretization methods with variable step-size in nonlinear wave digital structures for virtual analog modeling. IEEE/ACM Trans. on Audio, Speech, and Language Process., 27(11):1763–1776, Nov. 2019.*
- *D. Albertini, A. Bernardini, A. Sarti. Scattering Iterative Method based on generalized wave variables for the implementation of audio circuits with multiple one-port nonlinearities. In Proc. 150th Convention of the Audio Engineering (AES) Society, Online, May 25–28 2021.*
- *R. Giampiccolo, M. G. d. Bari, A. Bernardini, A. Sarti. Wave Digital Modeling and Implementation of Nonlinear Audio Circuits With Nullors. IEEE/ACM Trans. on Audio, Speech, and Language Process., vol. 29, pp. 3267-3279, 2021.*

Selected References

SIM with Dynamic Scattering Matrix Recomputation:

- *A. Proverbio, A. Bernardini, Augusto Sarti. Toward the Wave Digital Real-Time Emulation of Audio Circuits with Multiple Nonlinearities. In 2020 28th European Signal Processing Conference (EUSIPCO), pages 151–155, Amsterdam, The Netherlands, 2021.*

Selected References

Hierarchical SIM:

- *R. Giampiccolo, A. Bernardini, G. Gruosso, P. Maffezzoni, A. Sarti. Multiphysics Modeling of Audio Circuits With Nonlinear Transformers. Journal Audio Engineering Society, vol. 69, no. 6, pp. 374-388, (2021 June.).*
- *R. Giampiccolo, A. Bernardini, G. Gruosso, P. Maffezzoni, A. Sarti. Multidomain modeling of nonlinear electromagnetic circuits using wave digital filters. Wiley Int. Journal on Circuit Theory and Applications. 2022; 50(2): 539- 561.*

Parallel Hierarchical SIM:

- *R. Giampiccolo, A. Natoli, A. Bernardini, A. Sarti. Parallel Wave Digital Filter Implementations of Audio Circuits with Multiple Nonlinearities. Journal Audio Engineering Society, vol. 70, no. 6, pp. 469-484, (2022 June.).*

Selected References

Wave Digital Newton-Raphson:

- *A. Bernardini, E. Bozzo, F. Fontana, A. Sarti. A wave digital Newton-Raphson method for virtual analog modeling of audio circuits with multiple one-port nonlinearities. IEEE/ACM Trans. on Audio, Speech, and Language Process., 29:2162–2173, 2021.*

References I

[1] A. Fettweis. Wave digital filters: Theory and practice. *Proc. IEEE*, 74(2):270–327, Feb. 1986.

[2] A. Bernardini, P. Maffezzoni, and A. Sarti. Linear multistep discretization methods with variable step-size in nonlinear wave digital structures for virtual analog modeling. *IEEE/ACM Transactions on Audio, Speech, and Language Processing*, 27(11):1763–1776, Nov. 2019.

[3] R. C. De Paiva, S. D'Angelo, J. Pakarinen, and V. Välimäki. Emulation of operational amplifiers and diodes in audio distortion circuits. *IEEE Transactions on Circuits and Systems II: Express Briefs*, 59:688–692, Oct. 2012.

[4] A. Bernardini, K. J. Werner, A. Sarti, and J. O. Smith III. Modeling nonlinear wave digital elements using the Lambert function. *IEEE Transactions on Circuits and Systems I: Regular Papers*, 63(8):1231–1242, Aug. 2016.

References II

[5] A. Bernardini, K. J. Werner, J. O. Smith III, and A. Sarti. Generalized wave digital filter realizations of arbitrary reciprocal connection networks. *IEEE Transactions on Circuits and Systems I: Regular Papers*, 66(2):694–707, Feb. 2019.

[6] A. Sarti and G. De Sanctis. Systematic methods for the implementation of nonlinear wave-digital structures. *IEEE Transactions on Circuits and Systems I: Regular Papers*, 56: 460–472, Feb. 2009.

[7] T. Schwerdtfeger and A. Kummert. A multidimensional approach to wave digital filters with multiple nonlinearities. In *22nd Proc. European Signal Process. Conf.*, pages 2405–2409, Lisbon, Portugal, Sept. 1–5 2014.

References III

[8] T. Schwerdtfeger and A. Kummert. Nonlinear circuit simulation by means of Alfred Fettweis' wave digital principles. *IEEE Circuits and Systems Magazine*, 19(1): 55–C3, Firstquarter 2019. ISSN 1558-0830.

[9] Alfred Fettweis and Gunnar Nitsche. Numerical integration of partial differential equations by means of multidimensional wave digital filters. In *Proc. IEEE Int. Symp. Circuits Syst.*, pages 954–957, New Orleans, LA, May 1990.

[10] Muhammad Kabir, Carlos Christoffersen, and Nikhil Kriplani. Transient simulation based on state variables and waves. *International Journal of RF and Microwave Computer-Aided Engineering*, 21(3):314–324, 2011.

References IV

[11] Alberto Bernardini, Paolo Maffezzoni, Luca Daniel, and Augusto Sarti. Wave-based analysis of large nonlinear photovoltaic arrays. *IEEE Trans. Circuits Syst. I, Reg. Papers*, 65(4):1363–1376, April 2018.

[12] A. Bernardini, A. Sarti, P. Maffezzoni, and L. Daniel. Wave digital-based variability analysis of electrical mismatch in photovoltaic arrays. In *Proc. IEEE Int. Symp. Circuits Syst. (ISCAS)*, pages 1–5, May 2018. doi: 10.1109/ISCAS.2018.8351026.

[13] Alberto Bernardini, Kurt James Werner, Paolo Maffezzoni, and Augusto Sarti. Wave digital modeling of the diode-based ring modulator. In *Proc. 144th Audio Eng. Soc. Conv.*, Milan, Italy, May 24–26 2018. conv. paper #10015.

References V

[14] Alessandro Proverbio, Alberto Bernardini, and Augusto Sarti. Toward the Wave Digital Real-Time Emulation of Audio Circuits with Multiple Nonlinearities. In *2020 28th European Signal Processing Conference (EUSIPCO)*, pages 151–155, Amsterdam, The Netherlands, 2021.

[15] D. Albertini, A. Bernardini, and A. Sarti. Scattering Iterative Method based on generalized wave variables for the implementation of audio circuits with multiple one-port nonlinearities. In *Proc. 150th Convention of the Audio Engineering Society*, Online, May 25–28 2021.

[16] Carlos Christoffersen. Transient analysis of nonlinear circuits based on waves. In Luis R.J. Costa and Janne Roos, editors, *Scientific Computing in Electrical Engineering SCEE 2008*, pages 159–166. Springer Verlag, Berlin Heidelberg, 2010.

References VI

[17] Timothy Schwerdtfeger and Anton Kummert. Newton's method for modularity-preserving multidimensional wave digital filters. In *Proc. IEEE Int. Work. Multidimensional Syst.*, Vila Real, Portugal, Sept. 2015.

[18] L. Kolonko, J. Velten, and A. Kummert. Automatic differentiating wave digital filters with multiple nonlinearities. In *2020 28th European Signal Processing Conference (EUSIPCO)*, pages 146–150, Amsterdam, The Netherlands, 2021.

[19] M. J. Olsen, K. J. Werner, and J. O. Smith III. Resolving grouped nonlinearities in wave digital filters using iterative techniques. In *Proc. 19th Int. Conf. Digital Audio Effects*, pages 279–286, Brno, Czech Republic, Sept. 2016.

References VII

[20] Alberto Bernardini, Enrico Bozzo, Federico Fontana, and Augusto Sarti. A wave digital newton-raphson method for virtual analog modeling of audio circuits with multiple one-port nonlinearities. *IEEE/ACM Transactions on Audio, Speech, and Language Processing*, 29:2162–2173, 2021. doi: 10.1109/TASLP.2021.3084337.

[21] Granas A. and Dugundji J. *Fixed Point Theory*. Springer-Verlag, New York, 2003.

[22] William S. Hall and Martin L. Newell. The mean value theorem for vector valued functions: A simple proof. *Mathematics Magazine*, 52(3):157–158, 1979.